ISSN Application No. 21651

Journal of Mechanics and Thermodynamics

Volume No. 11
Issue No. 3
September - December 2023

ENRICHED PUBLICATIONS PVT. LTD

S-9, IInd FLOOR, MLU POCKET,
MANISH ABHINAV PLAZA-II, ABOVE FEDERAL BANK,
PLOT NO-5, SECTOR-5, DWARKA, NEW DELHI, INDIA-110075,
PHONE: - + (91)-(11)-47026006

ISSN Application No. 21651

Journal of Mechanics and Thermodynamics

Aims and Scope

Journal of Mechanics and Thermodynamics publishes theoretical and practice oriented papers, dealing with problems of modern technology (power and process engineering, structural and machine design, production engineering mechanism and materials, etc.), Materials and Design Engineering, Vibration and Control, Thermal Engineering and Fluids Engineering.

ISSN Application No. 21651

Journal of Mechanics and Thermodynamics

ISSN Application No. 21651

Journal of Mechanics and Thermodynamics

(Volume No. 11, Issue No. 3, September - December 2023)

Contents

Sr. No	Article/ Authors	Pg No
01	Analysis of Ductile-to-Brittle Transition Temperature of Stainless steel of 304 grades - *Mr. Sahadev Shivaji Sutar, Mr. Gorakshanath Shivaji Kale, Mr. Hrishikesh Sharad vaste*	109 - 118
02	P-Q theory based design of Unified Power Quality Conditioner for tranquillization of voltage and current unbalance under Non Linear Load condition. - *Mr. Jeevan J.Inamdar, Mr.Rahul S.Desai*	119 - 124
03	Finite Element Based Member Stiffness Evaluation of Axisymmetric Bolted Joint - *Mr. Chetan Chirmurkar, Prof. Mr. A. P. Deshmukh*	125 - 134
04	Case Study of Designing a Special Purpose Machine - *Prof. Prasad Bapat Prof. J. Y. Acharya*	135 - 140
05	Review of Heat Transfer Parameters using Internal Threaded Pipe Fitted With Inserts of Different Materials - *Mr. D.D.Shinde , Prof. A.M. Patil, Prof. H.M.Dange*	141 - 144

Analysis of Ductile-to-Brittle Transition Temperature of Stainless steel of 304 grades

[1] Mr. Sahadev Shivaji Sutar, [2] Mr. Gorakshanath Shivaji Kale, [3]Mr. Hrishikesh Sharad vaste

[1]Department of Mechanical Engineering, Solapur University / NBNSCOE, Solapur, India
sahadevsutar02@gmail.com
[2]Engg. Nath Pvt.Ltd. Hadapsar /Pune, Maharashtra, India
[3]Engg. Radheya Machining Ltd. Sanaswadi/Pune,Maharashtra,India
Rushikesh.vaste@rediffmail.com

ABSTRACT

The Ductile-to-Brittle Transition Temperature (DBTT) is a phenomenon that is widely observed in metals. Below critical temperature (DBTT), the material suddenly loss ductility and becomes brittle. The controlling mechanism of this transition still remains unclear despite of large efforts made in experimental and theoretical investigation. All ferrous materials (except the austenitic grades) exhibit a transition from ductile to brittle when tested above and below a certain temperature, called as Transition Temperature. The paper deals with the determination of the 'Ductile to Brittle Transition Temperature of stainless steel. Work carried out in this is purchasing the material followed by test specimen preparation. The specimens then keep in the liquid nitrogen for cooling for soaking time of 15 min. Then the actual charpy impact testing of the specimens at variable temperature ranging are carried out in controlled atmosphere. The readings taken are the impact energy (joules) of specimen at specific temperature. The graph of energy absorbed vs temperature is plotted to get the range of transition temperature.

This paper is a part of 3 papers analyzing the DBTT of

- *Stainless steel of 304grade*
- *Regular mild steel square rods*
- *Aluminum*

INTRODUCTION

NEED TO DETERMINE TRANSITION TEMPERATURE AND COMPARING

Why should steel that is normally capable of sustaining great loads and capable of ductility greater than 20 percent suddenly, when cold, become so brittle so brittle that it could be shattered a minor blow or similar impact? This was the question asked over a hundred years ago when fracture occurred in steel structures in severe structures in severe weather. Since then many similar failure have been documented. There are number of possible reasons for such failures:

- Fatigue.
- Corrosion.
- Fabrication.
- Design errors.
- Poor quality steel.

The most dramatic and unexpected cause of brittle failure in ferrous alloys is their tendency to lose almost all of their toughness when the temperature drops below their ductile to brittle transition

temperature. Between 1942 and 1952 around 250 large welded steel ships were lost due to catastrophic brittle failure. Another 1200 welded ships suffered relatively minor damage(cracks less than 10 feet long)while over 1900riveted ship have broken in two or lost at sea. Most of the failure occurred during the winter months. Failures occurred both when the ships were in heavy seas and when they were anchored at dock. These calamities focused attention on the fact that normally ductile steel can become brittle under certain conditions.

Fig.1 Liberty Ship & Brittle Fracture Seen In Liberty Ship

MAJOR ACCIDENTS HAPPENED IN INDIAN NAVY-

(Source: - http://en.wikipedia.org/wiki/List_of_Indian_Naval_accidents)

• **December 2013:** In the third incident in the same month, INS Tarkash (F50), again a Talwar class frigate, suffered damage to its hull when it hit the jetty while docking at the Mumbai naval base. The navy ordered a board of inquiry..

• **January 2014:** INS Betwa (F39), an indigenously built Brahmaputra class guided missile frigate, ran aground and collided with an unidentified object while approaching the Mumbai naval base. The sonar system of the frigate was cracked, leading to faulty readings and ingress of saltwater into sensitive equipment.

• **January 2014:** In the second incident in the same month, INS Vipul (K46), a veer class corvette of the elite 22nd Killer Missile Vessel Squadron, was detected with a hole in its pillar compartment which forced the ship back into the harbor while it was on an operational deployment.

• **March 2014:** INS Kolkata had a malfunction on board which led to a toxic gas leak killing Commander Kuntal Wadhwa instantly. It seems that the ship suffered malfunction in its carbon dioxide unit while undergoing machinery trials, leading to gas leakage. Since the ship was not commissioned at the time of the incident, the enquiry into the mishap will be done by Mazagon Dock Limited, where the ship was constructed.

From the above data we can observe that major accidents have been occurring in winter season for the above mentioned and such similar problem it becomes necessary to find out at what temperature the transition occurs and which material is best to use at cold atmosphere or at polar region. I.e. the material loses its toughness and ductility and loses its strength. The proposed project deals with finding out transition temperature and comparing strength of following material below room temperature and also below zero degree temperature.

FRACTURE MECHANISMS

At higher temperatures the yield strength is lowered and the fracture is more ductile in nature. On the opposite end, at lower temperatures the yield strength is greater and the fracture is more brittle in nature. This relationship with temperature has to do with atom vibrations. As temperature increases, the atoms in the material vibrate with greater frequency and amplitude. This increased vibration allows the atoms under stress to slip to new places in the material (i.e. break bonds and form new ones with other atoms in the material). This slippage of atoms is seen on the outside of the material as plastic deformation, a common feature of ductile fracture. When temperature decreases however, the exact opposite is true. Atom vibration decreases, and the atoms do not want to slip to new locations in the material. So when the stress on the material becomes high enough, the atoms just break their bonds and do not form new ones. This decrease in slippage causes little plastic deformation before fracture. Thus, we have a brittle type fracture. At moderate temperatures (with respect to the material) the material exhibits characteristics of both types of fracture. In conclusion, temperature determines the amount of brittle or ductile fracture that can occur in a material.

Another factor that determines the amount of brittle or ductile fracture that occurs in a material is dislocation density. The higher the dislocation density, the more brittle the fracture will be in the material.

The idea behind this theory is that plastic deformation comes from the movement of dislocations. As dislocations increase in a material due to stresses above the materials yield point, it becomes increasingly difficult for the dislocations to move because they pile into each other. So a material that already has a high dislocation density can only deform but so much before it fractures in a brittle manner. The last factor is grain size. As grains get smaller in a material, the fracture becomes more brittle. This phenomenon is due to the fact that in smaller grains, dislocations have less space to move before they hit a grain boundary. When dislocations cannot move very far before fracture, then plastic deformation decreases. Thus, the material's fracture is more brittle.

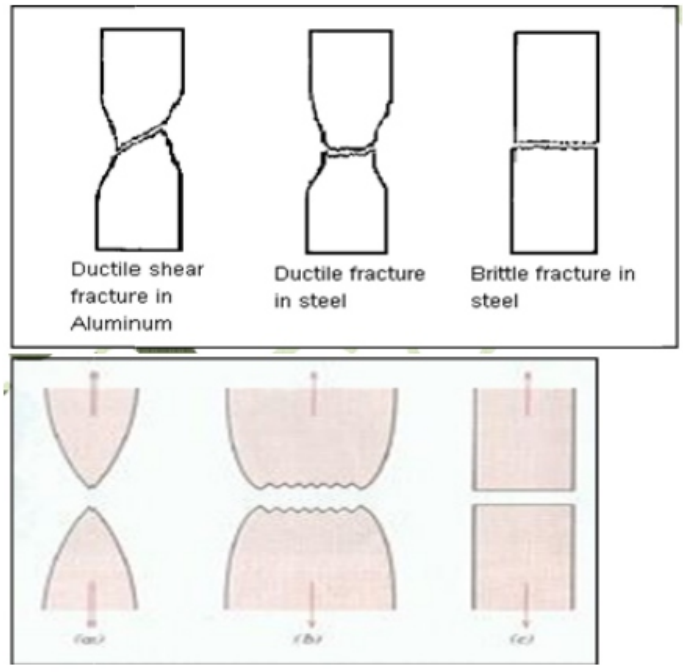

Fig 2 Ductile Fracture & Brittle Fracture Phenomenon

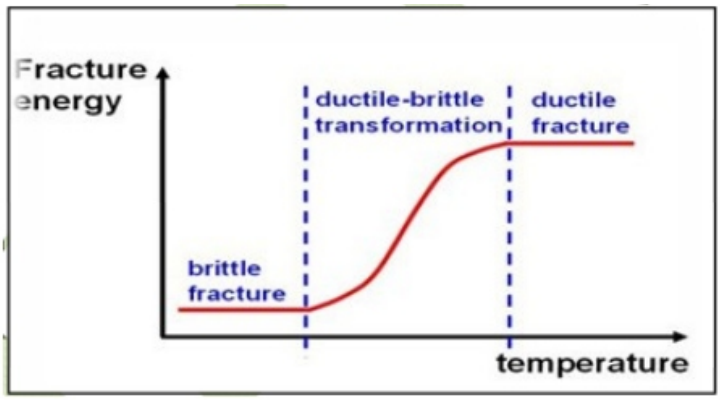

Fig 3. (A) Highly Ductile Fracture in Which Specimen Necks Down To a Point. (B) Moderately Ductile Fracture after Some Necking. © Brittle Fracture without Any Plastic Deformation.

Ductile to Brittle Transition temperature

The ductile-brittle transition is exhibited in bcc metals, such as low carbon steel, which become brittle at low temperature or at very high strain rates. FCC metals, however, generally remain ductile at low temperatures. In metals, plastic deformation at room temperature occurs by dislocation motion. The stress required to move a dislocation depends on the atomic bonding, crystal structure, and obstacles such as solute atoms, grain boundaries, precipitate particles and other dislocations. If the stress required moving the dislocation is too high, the metal will fail instead by the propagation of cracks and the failure will be brittle. Thus, either plastic flow (ductile failure) or crack propagation (brittle failure) will occur, depending on which process requires the smaller applied stress. In fcc metals, the flow stress, i.e. the force required to move dislocations, is not strongly temperature dependent. Therefore, dislocation movement remains high even at low temperatures and the material remains relatively ductile. In contrast to fcc metal crystals, the yield stress or critical resolved shear stress of bcc single crystals is markedly temperature dependent, in particular at low temperatures. The temperature sensitivity of the yield stress of bcc crystals has been attributed to the presence of interstitial impurities on the one hand, and to a temperature dependent Peierls- Nabarro force on the other. However, the crack propagation stress is relatively independent of temperature. Thus the mode of failure changes from plastic flow at high temperature to brittle fracture at low temperature.

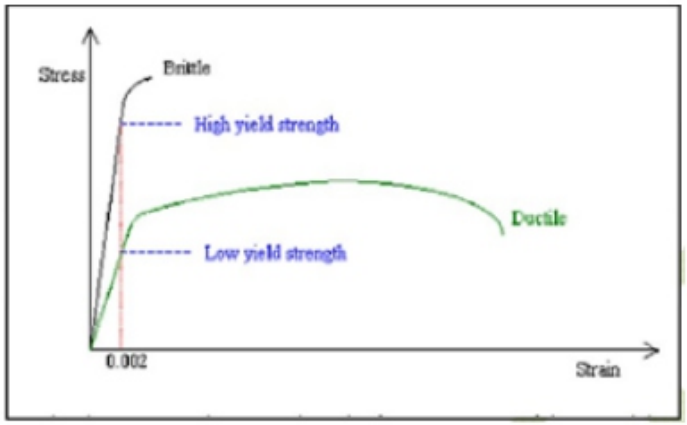

Fig 4 Ductile to Brittle Transition Graph

The ductile to brittle transition is characterized by a sudden and dramatic drop in the energy absorbed by a metal subjected to impact loading. This transition is practically unknown in fcc metals but is well

known in bcc metals. As temperature decreases, a metal's ability to absorb energy of impact decreases. Thus its ductility decreases. At some temperature the ductility may suddenly decrease to almost zero. This transition is often more abrupt than the transition determined by the energy absorbed. This temperature is called the nil-ductility transition temperature (NDTT). The NDTT is lower than the fracture energy transition temperature and is generally more narrowly defined. The difference between these two transition temperatures is related to the high rate of loading during impact testing rate sensitive metals. Increased loading rates cause the yield stress to increase while increasing temperature causes ductility to increase. .

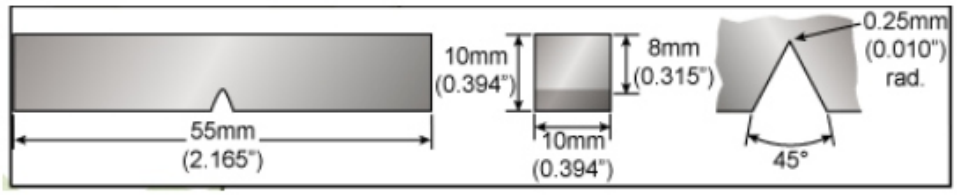

Fig 5 Typical Stress Strain Curve Of Steel.

Charpy Impact Testing (V-Notch)

The Charpy test is a three point bend impact test. It requires a specimen containing a machined notch in the center of the face facing away from the impacting device and a sturdy machine that can impart a sudden load to the specimen. The Charpy tester consists of a heavy pendulum which is allowed to strike the specimen at the bottom of its arch (maximum kinetic energy, maximum velocity). As the specimen deforms and fractures a portion of the kinetic energy of the pendulum is transferred to the specimen. The specimen is broken and the two pieces of the fractured specimen are knocked clear of the testing machine while the pendulum continues its swing to a somewhat lower position than it was released from. The difference in these heights and the mass of the pendulum determines how much energy was absorbed by the specimen. Most impact testers have a gage that reports this energy so that it doesn't have to be computed. Current applications of the Charpy impact test include comparisons of heat to heat variations of steel, evaluation of material behavior during either intentional or accidental high rates of loading, evaluation of the effect of irradiation on the embrittlement of steel, evaluation of the effects of microstructure and fabrication on toughness and studies of the fundamental aspects of deformation in bcc materials. Together the tensile test and Charpy impact test form a fairly complete evaluation of the mechanical properties of a material. However, it should be noted that the Charpy test is not a simulation of an alloy in service. The results of the Charpy tests are useful indications of how the material might behave in service.

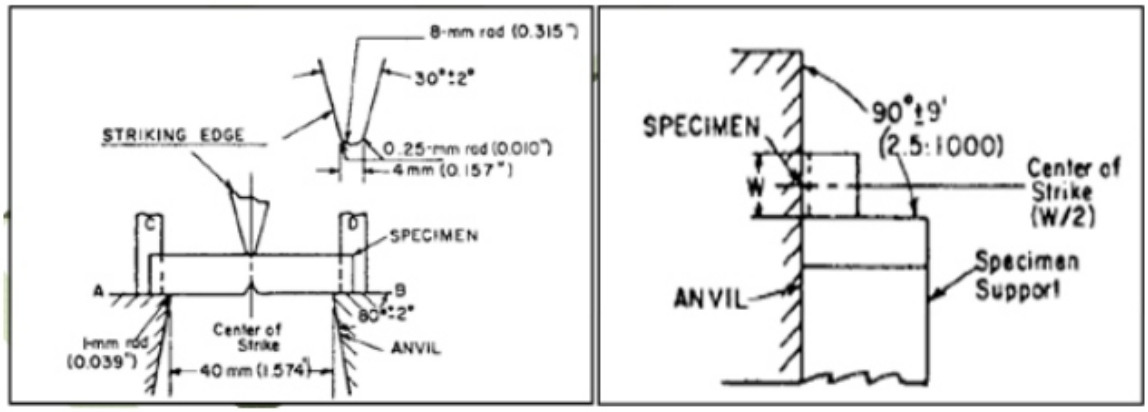

Fig 6 Typical Specimen for V-notch Charpy Test.

The Charpy impact test is a relatively simple, quick and inexpensive method for testing the dynamic fracture behavior of materials. It has been used extensively, particularly on ferrous alloys and has been standardized in ASTM E23.

Several of these, plus some additional guidelines are listed below.

This list should also provide some insight into the character of the Charpy impact test:

- The specimen cannot absorb more than 80% of the maximum energy capacity of the pendulum.
- The testing machine must be level and bolted securely to the floor.
- Alignment of the striker and the center of the specimen should be checked frequently.
- Slop in the axle and bearings should be within specified limits.
- The testing machine should be calibrated periodically. Wind age and friction should be checked Frequently.
- Specimen geometry, size, square and especially the acuity of the notch is critical. Variations of 0.005 inches in the depth of a V-notch can alter the results by 10 joules, almost 10 percent of the impact resistance of a tough material.

When conducting a test keep the following things in mind:

- The trigger mechanism should permit smooth release of the pendulum.
- The broken parts of the specimen must not interfere with the movement of the pendulum.
- No more than five seconds can elapse between the time the specimen is removed from then heating or cooling media until it is correctly seated in the specimen holder and tested.

One on the major drawbacks of the Charpy test is that it doesn't provide much information about the fracture process itself. Therefore, instrumented Charpy tests have been developed. A strain gage is mounted on the arm of the pendulum and a fast, triggered data acquisition system records the impact. The data provides load-time profiles that show the different stages of deformation and fracture: general yield, maximum load, fast fracture and arrest load after fast fracture. In addition, the actual energy absorbed can be obtained by accounting for the decrease in velocity of the pendulum as it fractures the specimen. An impact test can be used to assess a material's fracture resistance. Several such tests have been devised although in the United States the Charpy Impact Test is the one most widely used. In the Charpy test, a hammer is mounted on a very nearly frictionless pendulum. It is released from a specified height, h, and strikes the sample to be evaluated at the bottom of its arc. When it does so, the material is subjected to a high strain rate, which favors fracture rather than flow. Moreover, the notch on the specimen on the side of the bar subjected to impact tensile loading induces a triaxial state of stress in its vicinity and this also tends to promote fracture vis-à-vis flow. Thus, an impact test is associated with a high strain rate and a strong degree of triaxial loading, and as such it is a rather severe test of a material's toughness. Additionally, the sample test temperature can be varied, thereby allowing the determination of the temperature variation of the toughness.

ASTM – A370 Standards for Specimen Mounting

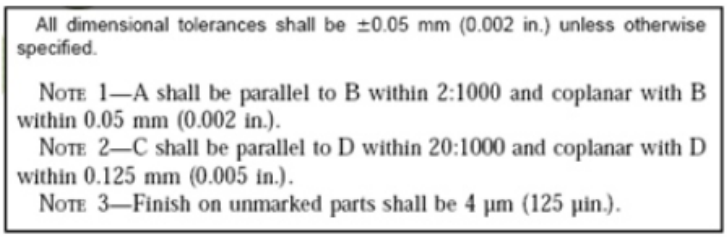
All dimensional tolerances shall be ±0.05 mm (0.002 in.) unless otherwise specified.

NOTE 1—A shall be parallel to B within 2:1000 and coplanar with B within 0.05 mm (0.002 in.).

NOTE 2—C shall be parallel to D within 20:1000 and coplanar with D within 0.125 mm (0.005 in.).

NOTE 3—Finish on unmarked parts shall be 4 µm (125 µin.).

MATERIAL SPECIFICATION

After studying the applications of various materials the material selected for DBTT determination are followingStainless steel of 304 grade STAINLESS STEEL OF 304 GRADE

Chemical composition-

Carbon	0.08 max.
Manganese	2.00 max.
Phosphorus	0.045 max.
Sulfur	0.030 max.
Silicon	0.75 max.
Chromium	18.00-20.00
Nickel	8.00-12.00 8.
Nitrogen	0.10 max.
Iron	Balance

Physical properties-

Specific Heat- (0 - 100°C) –0.50 kJ/kg K
Thermal Conductivity- W/mK (at 100°C) –16.2. (at500°C) 21.4
Density- 38.03 g/cm3
Magnetic Permeability- H = 200
Oersteds, Annealed - 1.02 max
Melting Range- (1399 °C – 1454°C)
Modulus of Elasticity- (MPa)
193 x 103 in tension
78 x 103 in torsion

Mechanical Properties-

Typical Room Temperature Mechanical Properties

UTS	0.2% YS	Elongation	Hardness
MPa	MPa	% in 2" (50.8 mm)	Rockwell
621	290	55	B82

Heat treatment-

Type 304 is non-hard enable by heat treatment. Annealing: heat to 1900 - 2050°f (1038 - 1121°c), then cool rapidly. Thin strip sections may be air cooled, but heavy sections should be water quenched to minimize exposure in the carbide precipitation region. Stress relief annealing: cold worked parts should be stress relieved at 750°f (399°c) for 1/2 to 2 hours.

SPECIMAN PREPERATION

The specimen for the charpy impact testing of required dimensions and tolerances are prepared as per ASTM A370 standards. The drawing of the specimen is as shown in fig Specimen have 10 *10 mm cross-section, 55mm length having a V-notch at centre. V-notch has 2mm depth and 45° notch angle.

NOTE 1—Permissible variations shall be as follows:

Notch length to edge	90 ±2°
Adjacent sides shall be at	90° ± 10 min
Cross-section dimensions	±0.075 mm (±0.003 in.)
Length of specimen (L)	+ 0, – 2.5 mm (+ 0, – 0.100 in.)
Centering of notch (L/2)	±1 mm (±0.039 in.)
Angle of notch	±1°
Radius of notch	±0.025 mm (±0.001 in.)
Notch depth	±0.025 mm (±0.001 in.)
Finish requirements	2 µm (63 µin.) on notched surface and opposite face; 4 µm (125 µin.) on other two surfaces

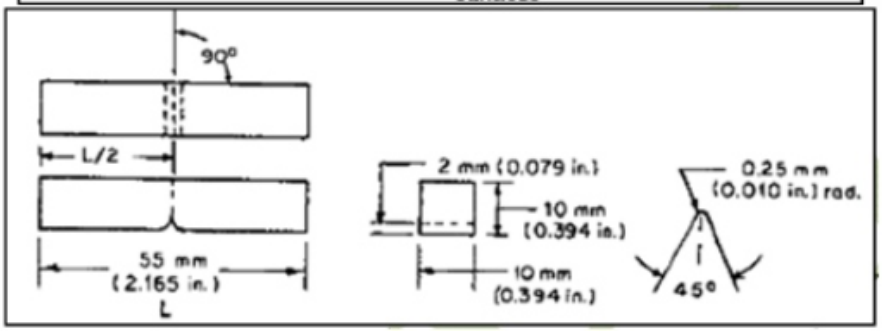

Fig 7 Specimen Drawing As Per ASTM A370 Standards.

EXPERIMENTAL PROCEDURE

Check that the operating of the impact testing machine is at the "Brake" position and that the Release stop is installed. Study the Charpy Impact Testing Machine and the two energy scales. The low-energy scale will be used for tests at 0°C and the high-energy scale for tests at temperature above 0°C.Practice the proper method to grip the specimen using the special purpose tongs provided. Also learn to mount the specimen properly in the impact testing machine. Turn the operating lever to "latch" position raise the pendulum to the lower energy or higher energy position depending upon the temperature at which the test is to be done. Keep all parts of your body well away from under the pendulum until the test is completed. Adjust the recording pointer on the energy scale such that it touches the moving pointer at the proper scale. Gripping a EN-19 specimen with the tongs' immerse it into the liquid nitrogen provided and hold until the liquid nitrogen stops boiling. Remove the specimen from the liquid nitrogen bath and, without any loss of time, mount it into the impact testing machine. Keeping a good distance from the machine, Turn the operating lever to "Release" position. The pendulum will swing down, hit the specimen, break it and swing up to the other side. Turn the operating lever to "Break" position. Read on the scale the value of the impact energy absorbed by the specimen for the fracture. Repeat the step 4 to 7 at the various temperatures. The temperatures can be achieved by immersing the specimen into constant temperature baths of liquid nitrogen, plain ice and boiling water. Repeat the steps 4 to 8 for the specimen of different alloys specified at the beginning

TEST TEMPERATURES

To attain the required temperatures for testing specimens was been kept in liquid nitrogen for soaking time of 10 min. After attaining required temperature, specimen was placed on anvil of test rig within 5 sec.

LIQUID NITROGEN -196°C
ROOM TEMPERATURE +35°C

Pendulum drop angle(degree)	140
Pendulum effective weight(kg)	21.300
Striking velocity of pendulum(m/sec)	5.308
Pendulum impact energy(joules)	300
Min. scale graduation(joules)	2
Distance between specimen anvils(mm)	40

Fig. 8 Impact Testing Machine & its Specifications

RESULTS

Experimental reading & graph for stainless steel grade 304

READING TABLE –

Sr. No	Temperature (In °C)	Energy absorb by specimen (in joule)
1	-120	-
2	-110	2.5
3	-100	3.5
4	-90	8
5	-80	24
6	-70	34
7	-60	26
8	-50	58
9	-40	82
10	-30	100
11	-20	105
12	-10	105
13	0	88

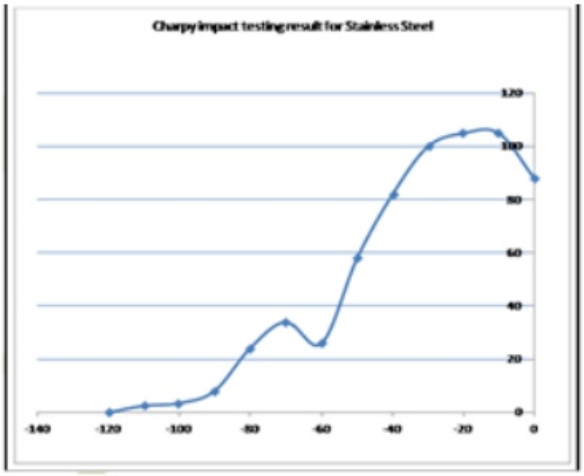

Graph for stainless steel grade 304

MICROSTRUCTURE IN DUCTILE BRITTLE REGION

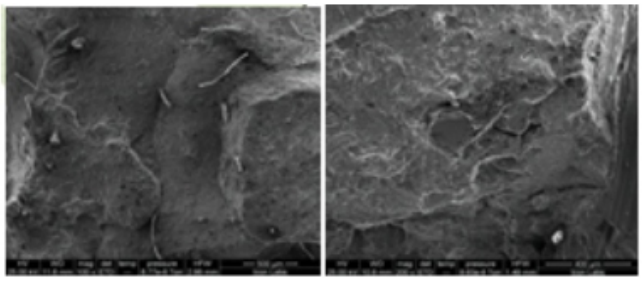

Fig 9.1 SEM Photograph Of Ductile Fracture at 100xFig 9.2 SEM Photograph of Ductile Fracture at 200x

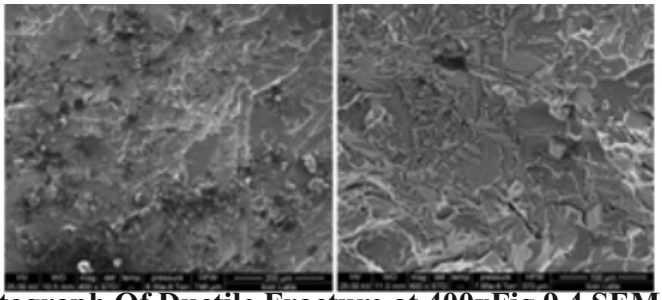

Fig 9.3 SEM Photograph Of Ductile Fracture at 400xFig 9.4 SEM Photograph of Ductile Fracture at 800x

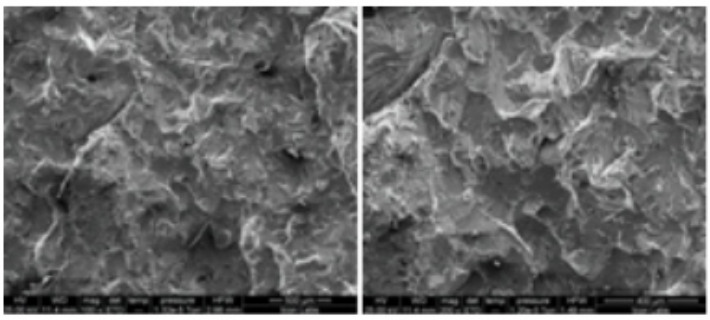

Fig 9.5 SEM Photograph Of Brittle Fracture at 100xFig 9.6 SEM Photograph of Brittle Fracture at 200x

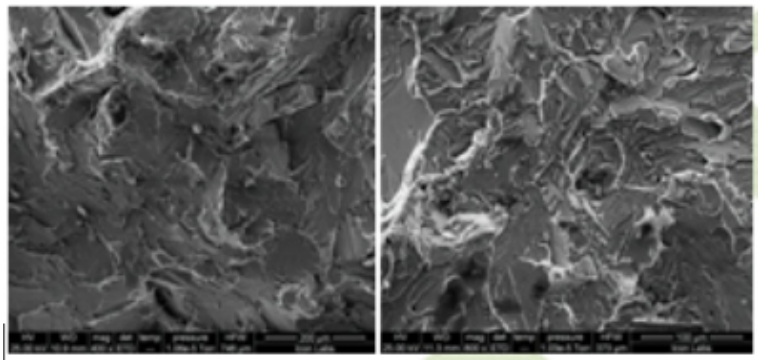

Fig 9.7 SEM Photograph Of Brittle Fracture at 400x Fig 9.8 SEM Photograph of Brittle Fracture at 800x

CONCLUSIONS

From above experimental results and graph we can conclude that for Stainless Steel- Energy absorb by specimen is very low between -90°C to -80°C so DBTT is in between -90°C to -80°C

REFERENCES

[1] B. Tanguy, J. Bensson R. Piques A.Pineau "Ductile to Brittle Transition of an A508 Steel Characteristics by Charpy Impact Test Part: I Experimental Result" Engng Fract Mech (2004) in press.

[2] Dr. Aniruddha moitra Material Technology Division "Study of Ductile-Brittle Transition Temperature of 9Cr-1Mo Steels".

[3] Alexande C. Edrington, Illinois institute of technology "Effect Of Intermediate Precipitation Treatments on The Temperature Embrittlement of 4140 Forging- Grade Steel".

[4] M.L. Hamilton and P.H.Jones "Effect of Heat Treatment and Test Method On DBTT Of V-5Cr-5Ti Alloy Steel"

[5] Standard Test Methods (Designation: A 370 – 02e) and Definitions for Mechanical Testing of Steel Products.

[6] Dr. V.D. Kodgire and S.V. Kodgire "Material Science and Metallurgy", Everest Publication. www.aksteels .com (for stainless steel 304) www.kleinmetals.ch (for mild steel) (Source: - http://en.wikipedia.org/wiki/List _of_Indian_Naval_accidents)

P-Q Theory Based Design of Unified Power Quality Conditioner for Tranquillization of Voltage and Current Unbalance Under Non Linear Load Condition.

[1] Mr. Jeevan J.Inamdar, [2] Mr.Rahul S.Desai

[1]Student - M. Tech., Electrical Department, BVDUCOE, Pune.411043, Maharashtra, India
g1inamdar@gmail.com,

[2]Assistant Professor, Electrical Department, BVDUCOE, Pune. 411043, Maharashtra, India
rsdesai@bvucoep.edu.in

ABSTRACT

This paper presents unified power quality conditioner (UPQC) which is an integration of shunt and series Active Power Filters and aims to compensate for voltage sag, voltage and current unbalance and other power quality problems [1],[5],[6]. The UPQC helps to improve power quality at the point of installation on power distribution system or industrial power system. This paper deals with design of UPQC by considering a controller based on PQ theory. Reference signal generation for shunt active filter is done by using PQ theory while for series dual PQ theory is used [2], [3]. Reference signals are then applied to pulse generators. Pulse generation is carried out by using hysteresis band controller for each filter. The validation of proposed scheme is carried out by using Matlab/Simulink.

Keywords – Unified Power Quality Conditioner, Active Power Filter, hysteresis control, voltage and current unbalance.

INTRODUCTION

With tremendous growth of power electronic industry and computer industry, the quality of power has become very poor. The main problem is the distortion of sine wave which causes voltage & current harmonics and thus affecting the performance of the equipment connected to the point of common coupling (PCC). Another problem is, it causes voltage unbalance at both ends of PCC thus affecting the operation of other loads connected to it [6]. The solution is Unified Power Quality Conditioner (UPQC) which is an integration of shunt and series active power filters [1]. The UPQC helps to compensate harmonic currents, imbalance due to non linear load, also harmonic voltages and imbalance of power supply.[5]

This paper focuses on heart of system, UPQC controller which generates pulses. For shunt active filter and series active filter the control (reference) signal is obtained by using instantaneous active and reactive power theory broadly known as P-Q theory. For series active filter dual P-Q theory is used which is converse of P-Q theory used for shunt active filter.[6] These control signals are then applied to pulse generators. Pulse generation is carried out by using separate hysteresis band controller for each filter. The paper represents design of control circuits for both techniques by using Matlab/Simulink. Lastly both filters are integrated to form UPQC which provides compensation for voltage unbalance, voltage sag and voltage harmonics, current harmonics.

UPQC

A. Block diagram

The general block diagram of UPQC is shown below which consists of shunt and series active filters with UPQC controller.

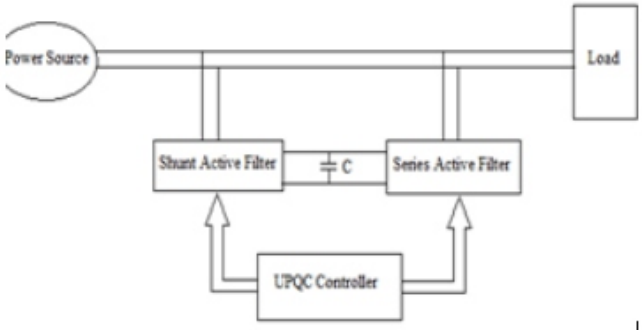

Fig. (a) Block diagram of UPQC

B. Proposed Scheme of UPQC controller

i. modelling equations for shunt and series active filter:

From measured values of phase voltages (Vp1, Vp2, Vp3) and load currents (iL1, iL2, iL3), controller calculates reference currents (i1r, i2r and i3r) used to produce compensation currents (ic1, ic2, ic3) and compensation voltages (vc1, vc2, vc3). This is accomplished by calculation of instantaneous active power P and instantaneous reactive power Q. This is well known as P-Q theory as explained below. [2], [3],[6].

Step 1:

• Clarke Transformation:

Calculation of $v\alpha$, $v\beta$, $i\alpha$ and $i\beta$

$$\begin{bmatrix} v\alpha \\ v\beta \end{bmatrix} = \sqrt{\frac{2}{3}} \begin{bmatrix} 1 & -\frac{1}{2} & -\frac{1}{2} \\ 0 & \frac{\sqrt{3}}{2} & -\frac{\sqrt{3}}{2} \end{bmatrix} \begin{bmatrix} Vp1 \\ Vp2 \\ Vp3 \end{bmatrix} \quad (1)$$

$$\begin{bmatrix} i\alpha \\ i\beta \end{bmatrix} = \sqrt{\frac{2}{3}} \begin{bmatrix} 1 & -\frac{1}{2} & -\frac{1}{2} \\ 0 & \frac{\sqrt{3}}{2} & -\frac{\sqrt{3}}{2} \end{bmatrix} \begin{bmatrix} iL1 \\ iL2 \\ iL3 \end{bmatrix} \quad (2)$$

Step 2:

• Instantaneous power calculation

Instantaneous real power

$$P = v\alpha . i\alpha + v\beta . i\beta \quad (3)$$

Instantaneous imaginary power

$$Q = v\alpha . i\beta - v\beta . i\alpha \quad (4)$$

Step 3:

The compensation signals are derived as follows:

a) Control method for shunt current compensation: [3],[6]

• α & β current calculations.

$$\begin{bmatrix} icα \\ icβ \end{bmatrix} = \frac{1}{vα^2 - vβ^2} \begin{bmatrix} vα & -vβ \\ vβ & vα \end{bmatrix} \begin{bmatrix} P \\ Q \end{bmatrix} \quad (5)$$

• **Inverse Clarke Transformation :** calculation of i1r, i2r and i3r (Reference current calculation)

$$= \sqrt{\frac{2}{3}} \begin{bmatrix} 1 & 0 \\ -\frac{1}{2} & \frac{\sqrt{3}}{2} \\ -\frac{1}{2} & -\frac{\sqrt{3}}{2} \end{bmatrix} \begin{bmatrix} icα' \\ icβ \end{bmatrix} \quad (6)$$

b) Series voltage compensation Control method by using dual P-Q theory. [6]

$$\begin{bmatrix} vcα \\ vcβ \end{bmatrix} = \frac{1}{iα^2 + iβ^2} \begin{bmatrix} iα & -iβ \\ iβ & vα \end{bmatrix} \begin{bmatrix} P \\ Q \end{bmatrix} \quad (7)$$

• Inverse Clarke Transformation : calculation of v1r, v2r and v3r (Reference voltage calculation)

$$\begin{bmatrix} v1r \\ v2r \\ v3r \end{bmatrix} = \sqrt{\frac{2}{3}} \begin{bmatrix} 1 & 0 \\ -\frac{1}{2} & \frac{\sqrt{3}}{2} \\ -\frac{1}{2} & -\frac{\sqrt{3}}{2} \end{bmatrix} \begin{bmatrix} vcα \\ vcβ \end{bmatrix} \quad (8)$$

ii. hysteresis controller

The hysteresis band control technique is used to generate the switching pattern of the inverter. The hysteresis control method is the best among other control methods, as it is quick controllable, easy to implement and unconditioned stability and easy to understand. It gives excellent dynamics and fastest control and requires minimum hardware.

.

Two-level hysteresis controller:

The pulses for both inverters are generated with the help of two level hysteresis controller by applying error signals to it. The error signal is derived by summation of reference signals and load side values. The output is applied to hysteresis controller to generate the pulses. For Positive sum the output switches to high and for negative or zero switches to zero, thus generating positive pulse train. The negation of this positive pulse train is done in order to generate negative pulses [7],[8].

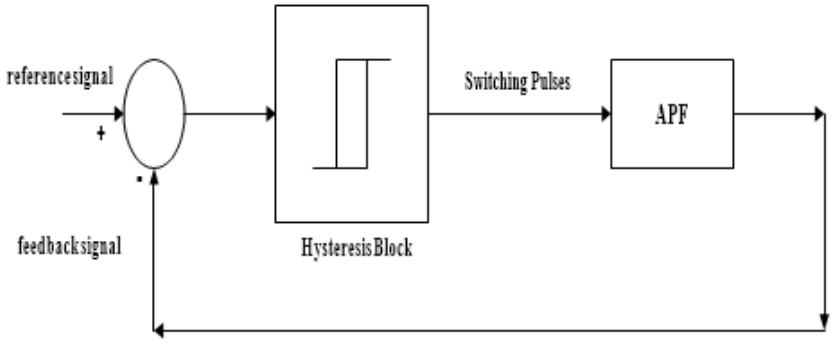

Fig. (b)Hysteresis controller block diagram.

iii. Shunt controller based on p-q theory

The matlab/simulink model is shown in Fig. (c)

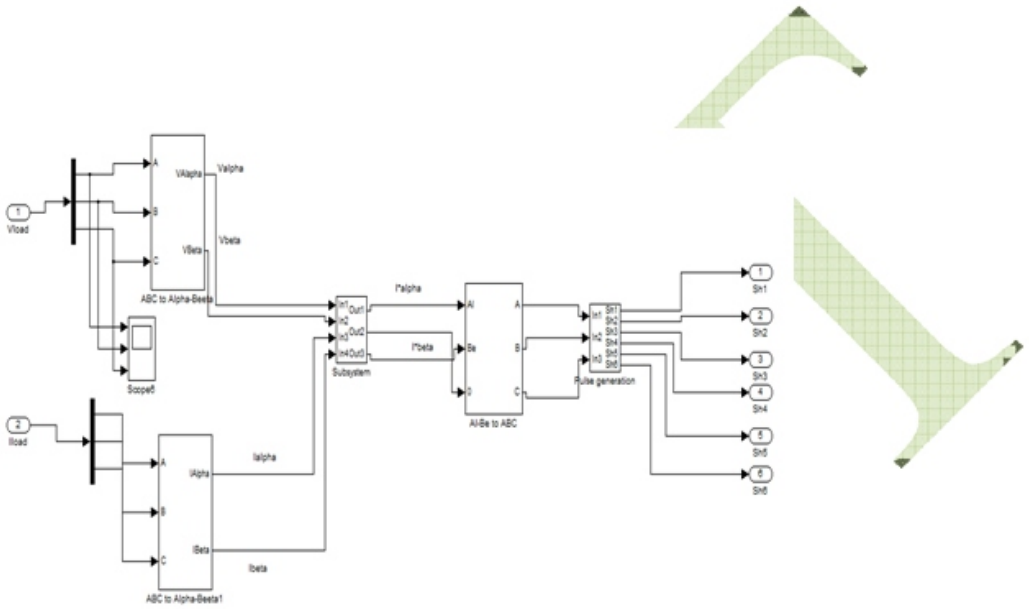

Fig. (c) Simulink model for shunt filter based on p-q theory.

iv. Series controller based on dual p-q theory

The matlab/simulink model is shown in Fig. (d)

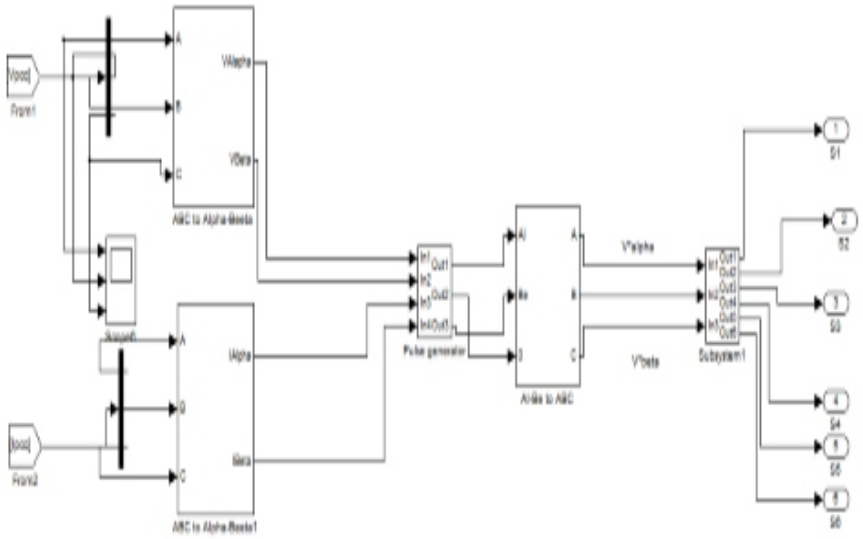

Fig. (d) Simulink model for series filter based on dual P-Q theory.

C. Simulation Results for UPQC :

The transition period for both circuit breakers is selected from 0.6 to 0.8. Two cases are considered. In first case when both filters are inactive, there is voltage unbalance and voltage sag at PCC as shown in Fig.(g) and Fig.(h) and when both are operated there is compensation as shown in Fig.(i) .For second case initial status is closed for shunt and series is open. This implies that initially shunt filter active giving load current compensation as shown in Fig. (f) While Fig. (e) Shows load current when shunt filter is inactive.

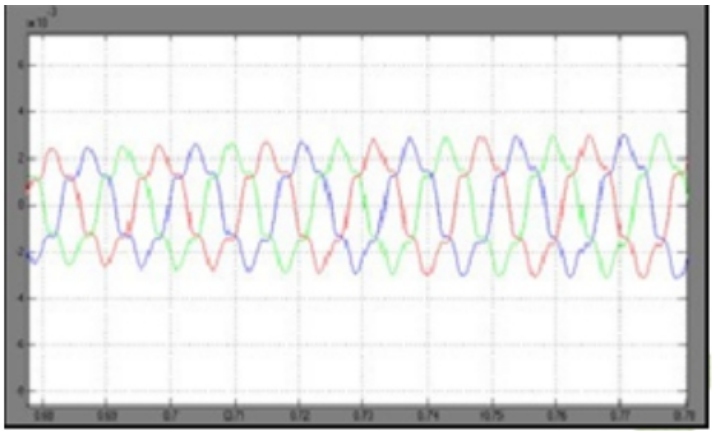

Fig. (e) Load current when shunt filter is inactive/

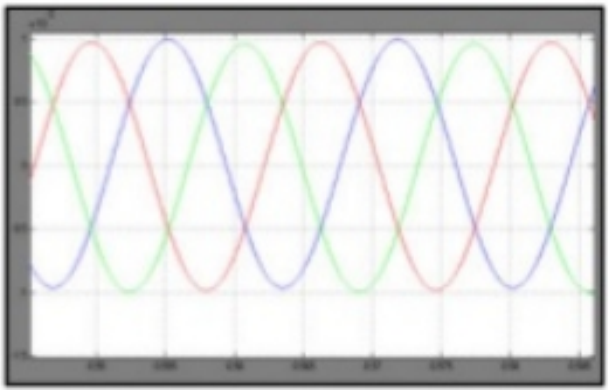

Fig. (f) Load current when shunt filter is operated.

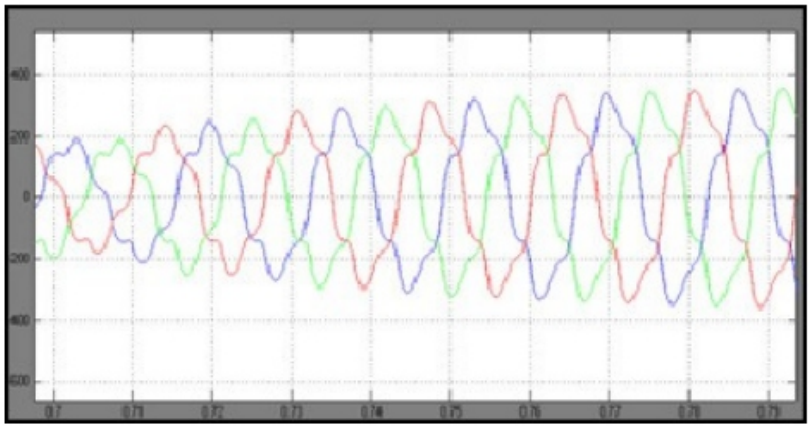

Fig.(g) Voltage at PCC before series filter is operated

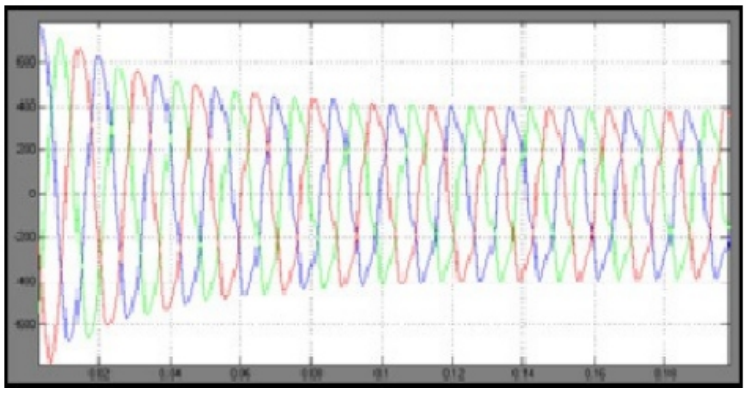

Fig.(h)Voltage sag observed at PCC before operation of series filter.

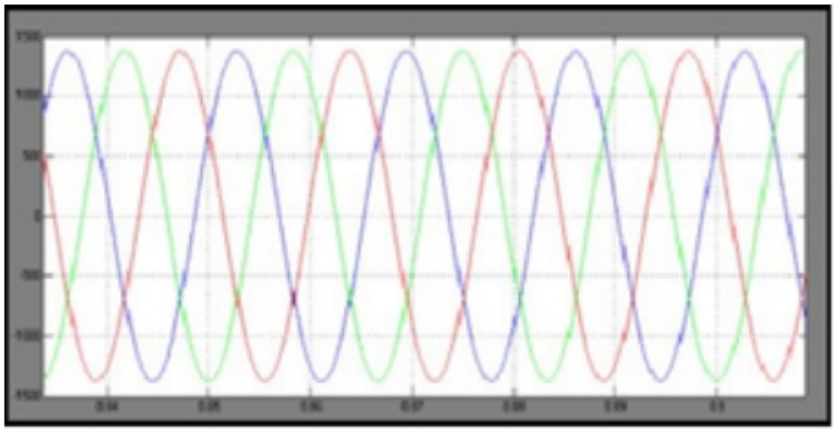

Fig.(I) Voltage at PCC after series filter is operated

CONCLUSION

This paper has focused on UPQC which aims at compensating not only current unbalance produced by non linear load but also voltage sag and voltage unbalance appearing at PCC. The control of UPQC is carried out by considering flow of instantaneous active and reactive power which is broadly known as P-Q theory. The simulation can further be modified to eliminate various power quality issues [5], [6].

REFERENCES

[1] H.Fujita and H.Akagi, "The Unified Power Quality Conditioner: The integration of Series – and Shunt –Active filters," IEEE Trans. on Power Electronics, vol.13, No.2, March 1998.

[2] H. Akagi, Y. Kanazawa, and A. Nabae "Generalized Theory of the Instantaneous Reactive Power in Three-Phase

Circuits," IPEC'83 - Int. Power Electronics Conf., Tokyo, Japan, 1983, pp. 1375-1386.

[3] J.Afonso , C.Couto and J.Martins , " Active filters with Control based on the p-q Theory ," IEEE Ind. Electronics Society Newsletter ,vol.47 , No. 3, Sept 2000, ISSN :0746-1240, pp.5-10.

[4] Vinod Khadkikar, "Enhancing Electric Power Quality Using UPQC: A Comprehensive Overview," IEEE Trans. on Power Electronics, vol. 27, no. 5, May 2012.

[5] H.Akagi, E.H. Watanabe and Maries, "Instantaneous Power Theory and Applications to Power Conditioning", IEEE press, A John Wiley & Sons, Inc., Publication, 2007

[6] R.C. Dugan, M.F. Mcgranaghan, Surya Santoso and H.Wayne Beaty, "Electrical Power Systems Quality", Second Edition.

[7] L. H. Tey, P. L. So, and Y. C. Chu, "Improvement of Power Quality Using Adaptive Shunt Active Filter," IEEE Trans. on power delivery, vol. 20, no. 2, april2005

[8] Fatiha Mekri, Mohamed Machmoum, Nadia Ait-Ahmed, Benyouness Mazari, "A comparative study of voltage controllers for series active power filter," ELSEVIER: Electric Power Systems Research 80 (2010) 615–626

Finite Element Based Member Stiffness Evaluation of Axisymmetric Bolted Joint

[1] Mr. Chetan Chirmurkar, [2] Prof. Mr. A. P. Deshmukh,

[1]Department Of Mechanical Engg. (Design Engg.), Savitribai Phule Pune University, D.Y.P.S.O.E. Lohegaon Pune, India chetanchirmurkar@gmail.com, chirmurkarchetan@yahoo.co.in

[2]Department Of Mechanical Engg. (Design Engg.), Savitribai Phule Pune University, D.Y.P.S.O.E. Lohegaon Pune, India

A B S T R A C T

For a reliable design of bolted joints, it is necessary to evaluate the actual fraction of the external load transmitted through the bolt. The stiffness of the bolt and the member of the joint decide the fractions of external load shared by the bolt and the member. Bolt stiffness can be evaluated simply by assuming the load flow to be uniform across the thickness and the deformation is homogeneous. Then, bolt may be modeled as a tension member and the stiffness can be easily evaluated. But, the evaluation of the member stiffness is difficult because of the heterogeneous deformation. In the present work, joint materials are assumed to be isotropic and homogeneous, and linear elastic axisymmetric finite element analysis was performed to evaluate the member stiffness. Uniform displacement and uniform pressure assumptions are employed in idealizing the boundary conditions. Wide ranges of bolt sizes, joint thicknesses, and material properties are considered in the analysis to evaluate characteristic behavior of member stiffness. Empirical formulas for the member stiffness evaluation are proposed using dimensionless parameters. The results obtained are compared with the results available in the literature.

Keywords- bolted joints, member stiffness, finite element analysis, axisymmetric model.

INTRODUCTION:

In engineering and day to day life, many cases arise when we have to join the two members. There are many joining methods used in engineering, as welding, brazing, soldering, and bolting. Each method has its own characteristics and use. For a particular case one of method is good and reliable, but for another cases it may worst or impossible. Bolted joints are used in abundance within the mechanical design of machinery. Most of these joints are noncritical to the overall success of a machine's function; nevertheless, a certain number of these joints are extremely critical and require in depth analysis for determining their acceptability. In automobile field and machineries, the bolted joints are famous. In bolted joints screw threads are used for tightening of two members. For tightening of members in bolted joints it require a bolt, it may be hexagonal or square but mostly hexagonal is preferred, and nut. It is as shown in fig.1

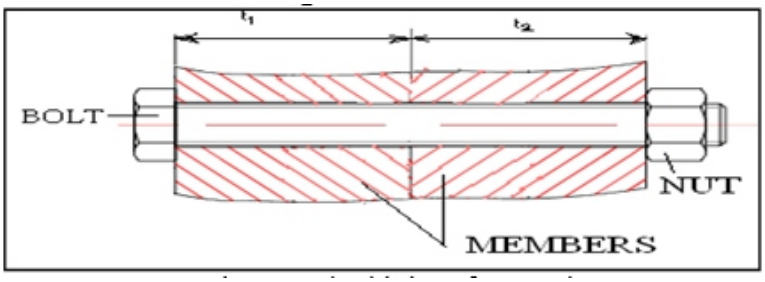

Fig.1 Bolted joint of a member

PRESTRESSING:

When it is necessary that the bolted member is joined enough strong to external force. So to tight the member prestressing is must. At the time of tightening extra torque is applied to the nut so that the member is compressedand due to which compression force (Fm) is acting on the member and tensile force (Fb) is generated in the bolt. The main two advantages of prestressing are it increase the fatigue life of the joints and it create a locking effect to the joints, it means the joint will not lose easily. The resultant loads acting on bolt and member is

$$F_B = \frac{Kb}{Kb+K_N} P + F_i \qquad (1)$$

K_m *and* K_b are stiffness of the member and bolt material which is

$$F_m = \frac{K_N}{Kb+K_N} P - F_i \qquad (2)$$

$$K_m = \frac{F_N}{\delta_N} = \frac{Æ_N E_N}{L} \qquad (3)$$

$$K_m = \frac{F_N}{\delta_N} = \frac{Æ_b E_b}{L} \qquad (4)$$

STIFFNESS:

Stiffness is load per unit displacement of any elastic member. In the previous article we have discussed about the calculation of the stiffness of the member as

$$K_m = \frac{F_N}{\delta_N} = \frac{Æ_b E_b}{L} \qquad (5)$$

If there are more than one member in joined by nut-bolt it assumed to be spring structure in series as shown in fig.2.

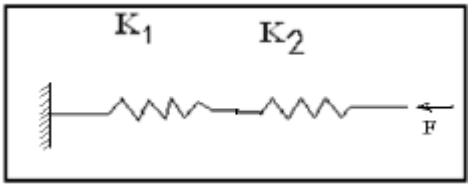

Fig .2 Stiffness model of member

The overall stiffness can be calculated,

$$\frac{1}{K} = \frac{1}{K_1} + \frac{1}{K_2} \qquad (6)$$

This formula is used when there is use of gasket in between the members and gasket is having stiffness less than other members, then other can be neglected for all practical purposes and only gasket stiffness is used. But if there is no gasket and if only a two member are joined by nut-bolt then it is difficult to calculate the joint stiffness, except by actual experimentation. Because deflection and force, area acting on the member is non uniform, it may be more at near the head and nut and low at the interface of two members.

In such cases where area under the compression are not known Prof. Charles Michke suggest the concept of pressure cone. Many analytical methods were proposed to calculate the area under the calculation but the pressure cone method is dominated. To model the actual system the conical shaped system is proposed. Prof. Michke propose the cone angle of 45^0

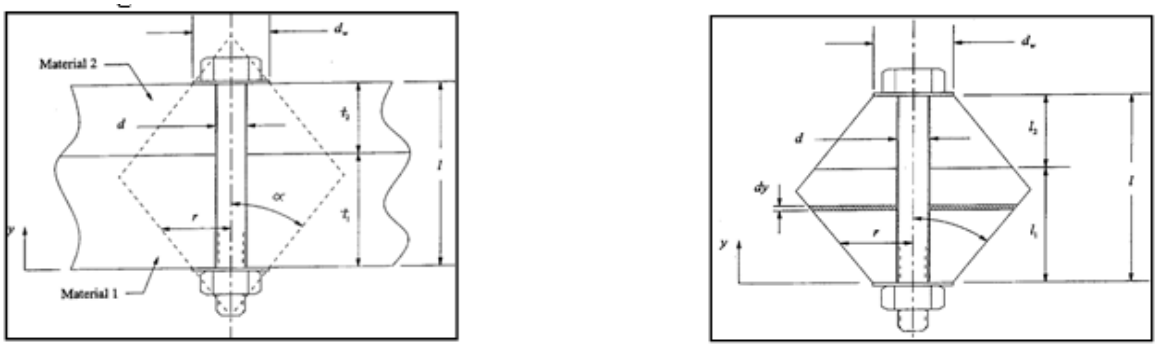

Fig.3 Cone geometry of bolted member

Fig.3 shows cone geometry, it has washer diameter dw, on both sides and joint of equal thickness member, this is assumed to simplify the case. But in actual there may be member of unequal thickness and may be more than one member of different modulus of elasticity. Shiglay [1] in his book assume $\alpha=45^0$.Later the same author proposed the angle as α=300.Verein Deutscher Ingenieur procedure consider it as $\alpha=30^0$.

The stiffness of frustum is given by Shiglay as

$$K_m = \frac{\pi E N d \tan}{2\ln\{\frac{(dw+L\tan\alpha-d)(dw+d)}{(dw+L\tan\alpha+d)(dw-d)}} \quad (7)$$

Assuming washer diameter $d_w=1.5d$, & $\alpha=30^0$ as best value

$$K_m = \frac{0.577\pi E N d \tan}{2\ln\{5X\frac{(0.577L+0.5d)}{(0.577L+2.5d)}} \quad (8)$$

The distinguishing characteristics of this system are cone angle'α', washer diameter 'dw', bolt diameter 'd' and clamped material thickness 'L'. Perhaps the most unsettled topic concerning this model has been the selection for the cone angle 'α', as the different author use different angle, no one has discussed relative important of choosing the proper value for this parameter. Verein Deutscher Ingenieur (VDI) procedure assumes α to be 30°. Juvinall and Marshek proposed the following expression to estimate the effective clamping area, Am, of the member.

$$A_m = \frac{n}{4}\left[\left(\frac{d2-d1}{2}\right)^2 - dh\right] \quad (9)$$

Where d_h=d for small clearance, $d_1=1.5d$, $d_2= d_1+L\tan\alpha$, and $\alpha=30^0$. Above equation is

$$A_m=d^2+0.68dl+0.065L \quad (10)$$

The stiffness of the member can be calculated by substituting above eq. in the equation of stiffness.

Apart from analytical models, many researchers used numerical methods such as finite element method to estimate member stiffness. Wileman et al performed axisymmetric finite element analysis (FEA) and proposed an exponential expression for member stiffness. In the analysis, the washer diameter dw was assumed to be 1.5 times the diameter of the bolt. They considered the displacement of the uppermost node located on the center line of the washer for stiffness calculation. Finite element analyses for various aspect ratios (dh L) were carried out and finally an exponential relation for member stiffness evaluation was proposed. This is as below,

$$Km = Em\ dh\ A e^{Bdh/S} \quad (11)$$

Where,

A, B = material constants.
A = 0.78952 and B=0.62914

Which valid for engineering materials such as steel, copper, aluminum, and cast iron. This formula is mostly applicable for the cases with dh /L≤ 2 and shown to be quite simple and efficient method to calculate the member stiffness. Later many researchers used and developed the same technique to evaluate the member stiffness. The work is proposed an exponential relationship using no dimensional geometric and material parameters for member stiffness evaluation. The analysis was done using finite elements considering various bolt sizes, geometries, and different member materials. Most of the methods presented in the literature review have differences in the results. The differences in the results are mainly due to the assumptions made during the model development. This is value of pressure cone angle and confined uniform stress field in a particular region. Manring [3] showed the member stiffness dependents on the choice of cone angle. The differences caused by various assumptions need higher safety factors for reliable design. Wileman formula, given in Eq. (11), is an attempt to handle the inaccuracies but the formula itself is restricted to limited variation of parameters. In this, we are doing an attempt to carry out systematic study and evaluation of member stiffness for various geometric and material properties of the joint members. An ideal condition are considered where effects of member diameter, thread friction, contact friction between bolt head/washer and members, interface slip between members, and external shear loads are not considered in the present analysis; hence all such effects if present should be compensated by proper safety factor. The proposed formulas should not be applied for joints in which members may subject to very high external loads and tend to separate from each other.

METHOD OF APPROACH:

Our main aim is to propose a formula for member stiffness evaluation based on the results of linear finite element analysis. The member stiffness is calculated using finite element method and it is divided by a stiffness measure Ko to get a dimensionless quantity R, called "correction factor," as given by

$$R = \frac{K(FEM)}{K0} \quad (11)$$

$$K_o = \frac{\pi E_m}{4L}(d_w^2 - d_h^2) \quad (12)$$

Where,

Ko=the stiffness of hollow cylinder with internal and external diameters the same as that of the washer and length equal to the joint thickness.

If, Ko = KFEM , then R=1

So we are comparing the KFEM to the stiffness of the hollow cylinder with internal and external diameters the same as that of the washer. Correction factors for various joint geometries and material constants are obtained by detailed parametric finite element analysis and empirical relations to calculate the correction factor are proposed by least squares curve fitting.

Finite Element Modeling and Analysis:

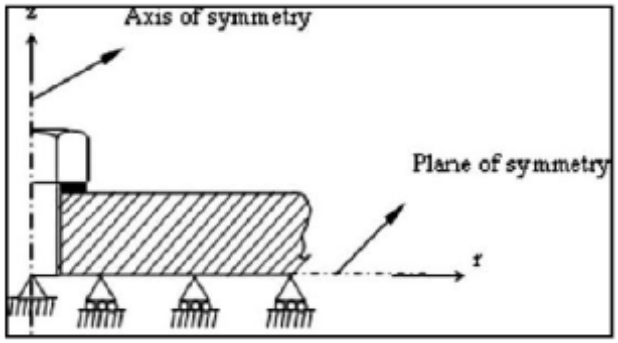

Fig. 4 Axisymmetric half model of the bolted joint

For the finite element modeling of the bolted joint, the assumptions made are

1) The geometry of the joint is assumed to be perfectly Axisymmetric.
2) The two members of the joint are assumed to be made of the same material and have the same thickness,
3) Also assumed to be in perfect contact without slippage.
4) The effect of screw threads is ignored.
5) The member material is assumed to be homogeneous, isotropic, and linearly elastic.

Due to the second assumption, the two members of the joint can be treated as a single continuous member and planar symmetry about the joint midplane is introduced in the model. Both the symmetries are incorporated in the model by applying proper symmetry constraints, as shown in Fig. 4. Commercial finite element software ANSYS is used for modeling and analysis. To avoid the edge effects, the outer diameter of the member is taken to be five times the diameter of the bolt hole. The model is meshed by eight noded axisymmetric quadrilateral elements. A schematic finite element discretization is shown in Fig.5. The member material is assumed to be homogeneous, isotropic, and linearly elastic with Young's modulus, Em, equal to 210 GPa, for all the analyses.

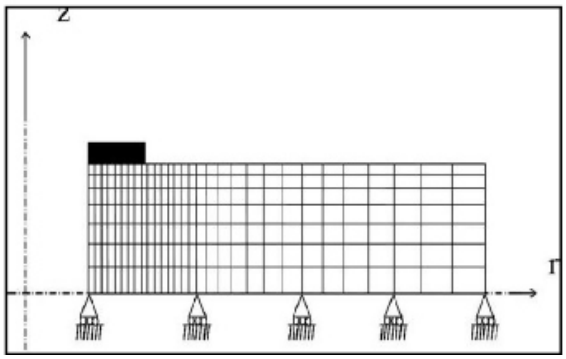

Table 1 List of bolt sizes and related dimensions

Bolt size	Bolt diameter d (mm)	Hole diameter d_h, $d_h = d + 2c$ (mm)	Washer diameter d_w, $d_w = 1.5d$ (mm)
M6	6	6.5	9
M8	8	8.5	12
M10	10	10.5	15
M12	12	13	18
M16	16	17	24
M20	20	21	30
M24	24	25	36
M30	30	31	45
M36	36	37	54

Fig. 5 Schematic finite element mesh

The outer diameter of the washer is taken to be 1.5 times the Diameter of the bolt, i.e., same as the diameter of the bolt head (distance between flats of metric hexagonal bolt head). Dimensions of various bolts and corresponding washers used in the analysis are given in Table 1.

BOUNDARY CONDITIONS:

1) E1=E2
2) t1=t2=l/2
3) Plane of symmetry is steady i.e. plane of symmetry is remains plane after deformation.
4) Force applied at top

In this work, the load transfer is simulated by two different assumptions, which are explained below and the results obtained from both the assumptions are compared.

UDA:

This case corresponds to a joint in which the washer is highly rigid (hard washer) compared with the member. Due to this, the displacement of member under the washer is almost uniform. This condition is realized in the finite element analysis by applying a predetermined axially downward uniform displacement to the topmost nodes, which fall within the outer diameter of the washer. The sum of the upward reactions, Fr, of the nodes below the washer is divided by twice the applied displacement (due to symmetry) to get the stiffness of the member.

The stiffness is given by

$$K_{FEM} = \frac{pA_w}{2\delta_a} \tag{14}$$

Where A_w is the area under the washer and is given by

$$A_w = \frac{\pi}{4}(d_w^2 - d_h^2) \tag{15}$$

The average nodal displacement is used for calculation of KFEM only for UPA because the displacement field under the washer contact area is varying in the radial direction with a maximum value at the bolt hole and a minimum value at the outer edge of the washer. Longitudinal stiffness also varies along the radial direction. From the mean value theorem, for constant pressure boundary conditions, the average displacement gives the member stiffness in an average sense. Earlier, Lehnhoff et al. also used average displacement of nodes below the bolt head to calculate the member stiffness.The uniform displacement assumption (UDA) corresponds to the finite element boundary condition where the washer is assumed to be highly rigid compared with the member and the uniform pressure assumption (UPA) corresponds to the boundary condition where the washer is assumed to be very soft compared with the member. Plots of displacement contours of a 40 mm thick joint with M20 bolt with UDA and UPA are shown in Figs. 6 and 7, respectively.

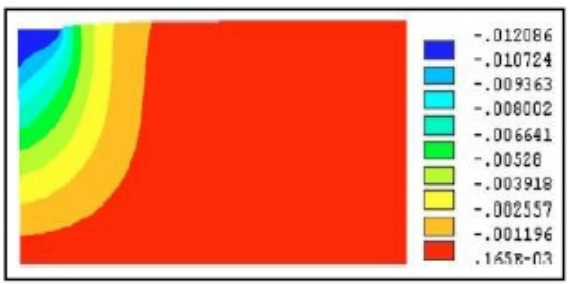

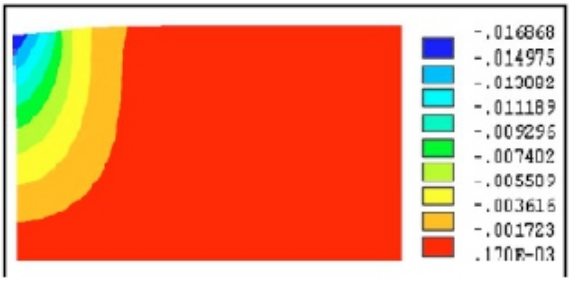

Fig.6Displacement contours with UDA(M20 joint, L=40 m)
Fig.7Displacement contours with UPA (M20 joint,L=40 m)

In the actual joint neither the displacement nor the contact pressure below the washer is uniform. The idea behind using the assumptions for preload simulation is to calculate two different estimates of member stiffness, which will work as upper and lower bounds and the actual value of member stiffness will be in between the limits when the analysis is carried out with the actual washer stiffness.

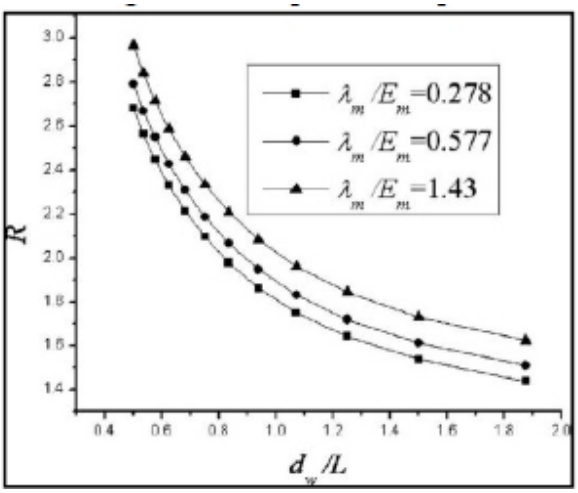

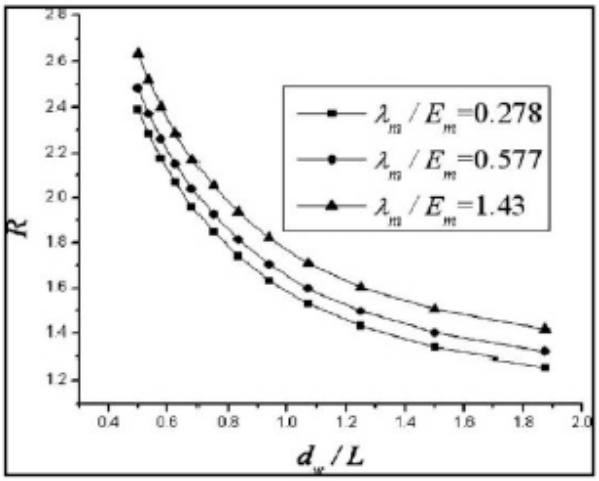

Fig. 8 Variation in R with dw/L for bolt size M20 (UDA) Fig. 9 Variation in R with dw/L for bolt size M20 (UPA)

The assumptions of UDA and UPA may give (not proved in the present study) the upper and lower bounds of the member stiffness pertaining to the material rigidity of the washer relative to the member. In practice, the washer will have stiffness, which may not be very rigid or soft, and the rigidity will be of finite values. Convergence study is carried out on the initial finite element model by decreasing the element size and converged model with element edge length of 0.33 mm is used for the rest of the Analysis. The number of elements used in the analysis is not constant due to change in geometry. The number of elements used in the converged analyses ranges from 1000 to 40,859.

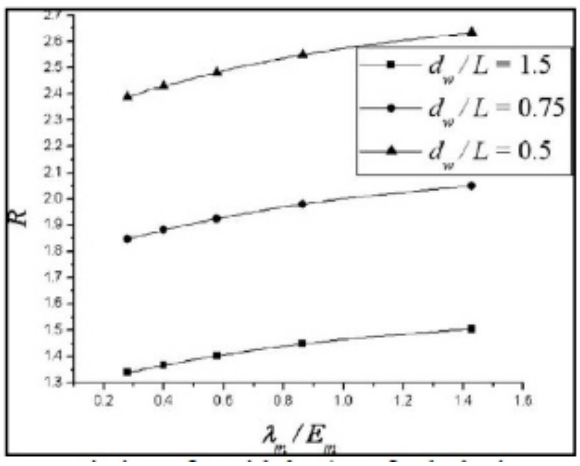

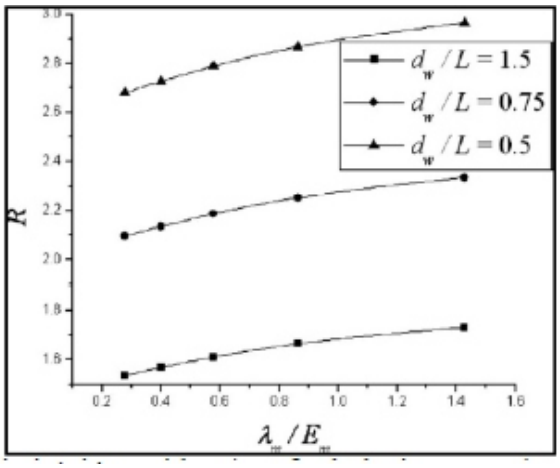

Fig.10Variation of Rwith λm/Em for bolt size M 20 (UDA)
Fig.11Variation in R with m/Em for bolt size M 20 (UPA)

RESULTS AND DISCUSSION:

Parametric study is carried for nine different bolts ranging from M6 to M36 with joint thickness ranging from 16 mm to 60 mm with an increment of 4 mm and with five different Poisson ratio values varying from 0.2 to 0.4 with an increment of 0.05 for both UDA and UPA boundary conditions. The number of converged case studies conducted for each of UDA and UPA is 540. Correction factors are calculated for all the case studies using Eq.(11) used above. The finite element stiffness values for various bolt sizes and joint geometries are given in reference [4], but one of it are given in Tables 3.

Empirical Relation for Correction Factor: It is observed from the results of FEA that the stiffness of the member isdependent on the dimensions of the bolt hole, washer diameter, and grip length of the joint. Along with these three factors, the Member stiffness is also dependent on Lamé's constant of the member material, λm. This is because when the member is axially compressed by the load, the member below the washer will try to expand in radial direction due to Poisson's effect and the material around the washer will restrict this expansion due to which radial stresses are induced in the member. These stresses, which influence the member stiffness, are observed to be proportional to Lamé's constant. Therefore, the following dimensionless parametric group is used to express the correction factor.

$$R = f\left(\frac{d_w}{d_h}, \frac{d_w}{L}, \frac{\lambda_m}{E_m}\right) \qquad (16)$$

As metric standard bolt dimensions are used throughout the analysis, dw/dh is nearly constant and retained in the expression only to represent the effects of bolt hole clearance. Variation in correction factor with dwL is shown in Figs. 6 and 7 for UDA and UPA, respectively. In each plot, it can be observed that the curves resemble exponential decay pattern. Figures 8 and 9 show that the correction factor increases with increase in λmEm (ratio is a function of Poisson's ratio). Finally, an empirical relation for correction factor was proposed after observing the variation with individual variables of Eq. (16) and using a least squares curve fitting algorithm. During the initial curve fitting process, the curve was assumed to be of the form, exponential proposed by Wileman et al. In our modeling, three non dimensional parameters (dw/dh, dw/L, and λmEm) are introduced to account for the wide range of geometric and material parameter variations. Later, the correction factor (R) variation is characterized for different geometrical non dimensional parameter variations for a given material property value. It was found that use of powers of non dimensional variables (dw/dh)c1(dw/L)C2 fitted the curve well. The process was repeated for different material property values (λmEm). Finally, it was observed that the introduction of inverted hyperbolic function allowed fitting all the results into a single curve with minimal error (less than 3%). The final expression for correction factor is given by

$$R = C5 + C6 \exp(S) \qquad (17)$$

Where S is an intermediate variable used for convenience of expression and it is given by

$$S = C_4 \quad \sinh^{-1}((dw/dh)^{c1}(dw/L)^{C2}) + (hM/EM)^{C3} \qquad (18)$$

The constants used in Eqs(17) and (18) for UDA and UPA are given in Table 2. The maximum error in curve fitting is below 3% for both UDA and UPA.The member stiffness for any arbitrary joint geometry can now be calculated using the proposed empirical formula. However, it is very important to carefully review the inherent assumptions used to obtain this formula before using it, particularly the preload simulation methods using UDA and UPA. As explained earlier, both the assumptions are extreme idealizations of the actual phenomenon. Accordingly, the stiffness obtained by UDA always predicts the higher value for the member stiffness than that obtained by UPA. The selection of the appropriate assumption should be made depending on the problem at hand. The diameter of the washer is taken to be equal to the bolt head diameter (1.5 times the diameter of bolt) in the present work. As the diameter of the washer influences the member stiffness, these formulas should not be used if the difference between the washer diameter and the bolt head diameter is considerable. In the case of a joint without washer, formula can be used by replacing washer diameter by bolt head diameter.It is observed in the present work that the member stiffness is increased by 8–13% approximately with the increase in (λmEm)(as (λmEm) is a function of Poisson ratio) alone) from 0.28 (μ =0.2) to 1.43(μ =0.4), see Figs. 10 and 11. This variation was accounted for in the proposed empirical formulas.In this work, the outer diameter of the member, dm, is taken to be five times the diameter of bolt hole, dm, to avoid the edge effects. Except for very small values of dw/L, increase in member diameter beyond 3.5 times dh results in a negligible increase in stiffness, see Fig. 10. It is also evident from Fig. 10 that the member stiffness decreases steeply with a decrease in the member diameter beyond three times dh. Hence the proposed formula can be safely used for member diameters starting from 3.5 times dh .

Table 2 Empirical constants used in correction factor expression

Constant	UDA	UPA
C_1	−1.9690	−2.0417
C_2	−1.0831	−1.1605
C_3	0.051039	0.048737
C_4	0.69997	0.65097
C_5	−0.66075	−0.67007
C_6	0.69004	0.64828

CONCLUSIONS:

In the present work, the member stiffness of bolted joints is calculated using the axisymmetric finite element analysis and an empirical formula for the computation of member stiffness is proposed. The external load on the joint member is applied using UDA and UPA. Parametric study has been carried out for different bolts ranging from M6 to M36, joint thickness ranging from 16 mm to 60 mm, and Poisson ratio varying from 0.2 to 0.4. It is observed that the member stiffness varies by 8–13% with an increase in Poisson's ratio from 0.2 to 0.4. The proposed empirical formulas fit very well with the finite element simulations and the maximum deviation observed was less than 3%. Finally, the results are compared with the results obtained from previous methods in the literature and it is observed that the reported results overestimate the stiffness. The overestimation of the member stiffness for the conical clamp analytical model is mainly due to the cone angle selection. Selecting a lower cone angle may give better estimates of the stiffness.

NOMENCLATURE:

A, B = material constants
C = radial clearance
D = nominal diameter of the bolt
L = grip length/thickness of the joint
Pext = external load
p = uniform pressure applied on the nodes under washer
R = correction factor
S = intermediate variable
r, z = radial and axial coordinates
α = semivertex angle of the frustum of pressure cone
δ = boundary displacement applied on the nodes under washer
μ = Poisson ratio
Ab = nominal cross sectional area of the bolt shank
Am = effective clamping area
Aw = area under the washer/bolt head in the case of no washer
Ci = constants used in correction factor expression, the subscript i vary from 1 to 6
dh = diameter of bolt hole or washer inner diameter
(dh=d+2c)
dm = outer diameter of the member
dw = washer outer diameter/bolt head diameter in the case of no washer
d1, d2 = minor and major diameters of the conical frusta
Eb = elastic modulus of bolt material
Em = elastic modulus of member material
Fb, = fraction of external load acting on bolt
Fi = preload applied on the joint
Fm = fraction of external load acting on members
Fr = sum of reaction forces of nodes under washer in UDA
Kb = bolt stiffness
KFEM = member stiffness, calculated by finite element analysis
Km = member stiffness
Ko = stiffness of hollow cylinder with inner and outer diameters as that of washer and length equal to the thickness of the joint.
δa = average displacement of nodes under washer
δb = effective elongation of bolt due to preload
δm = effective compression of member due to preload

REFERENCES:

[1] Shigley, J. E., and Mitchell, L. D., 1983, Mechanical Engineering Design, 4thMcGraw-Hill, New York.
[2] Norton, R. L., 2000, Machine Design, An Integrated Approach, 2nd Edition, Prentice Hall, Upper Saddle River, New Jersey.
[3] Manring, N. D., 2003,Sensitivity Analysis of the Conical Shaped Equivalent Model of a Bolted Joint," ASME J. Mech. Des., 125, pp. 642–646.
[4] Sethuraman R.,Sasi Kumar T.,2009," Finite Element Based Member Stiffness Evaluation of Axisymmetric Bolted Joints"ASME J. MECH. Des.131,
[3] Abdel-Hakim Bouzid, Hichem Galai, "A New Approach to Model Bolted Flange Joints With Full Face Gaskets", ASME J. Mech. Des
[4] Abdel-Hakim Bouzid, Hichem Galai, "A New Approach to Model Bolted Flange Joints With Full Face Gaskets", ASME J. Mech. Des
[5] Sayed A. Nassar, Antoine Abboud , "An Improved Stiffness Model for Bolted Joints", ASME J. Mech. Des

Case Study of Designing a Special Purpose Machine

[1] Prof. Prasad Bapat, [2] Prof. J.Y. Acharya

[1]Department of Mechanical, Mumbai University / MPCOE, Velneeshwar, India,
prasad.rbgi@gmail.com

[2]Department of Mechanical, Mumbai University / RSCOE, Chiplun, India

ABSTRACT

Special purpose machine tools are designed and manufactured for specific jobs and such never produced in bulk such machines are finding increasing use in industries the techniques for designing such machine would obviously be quite different from those used for mass produced machine. A very keen judgment is essential for success of such machines. This paper explains a case study of designing special purpose machine and manufactured at ABC Company which found beneficial in increasing production quantity & reducing manpower.

KEYWORDS: - SPM, LOCUS CLEARANCE, MACHINE HEAD, CASTINGS BLOCKS

INTRODUCTION TO SPECIAL PURPOSE MACHINE

Broadly the special purpose machine tools could be classified as those in which jobs remain fixed in one position and those in which job moves from one station to other (Transfer machine).In first case the machine may perform either only one operation or more .In the second case, the product may be either moving continuously (as in the case of spraying, polishing, sanding etc) or intermittently (the most usual case in machining operation). Rotary intermittently motion transfer machine is very popular production machine and is described in brief bellow. Such a machine comprises a turret on whole periphery several heads are mounted to receive and locate the components for working. The turret rotates intermittently about its central axis which is provided with fine and sophisticated mechanisms to control its motion so that before stopping it is properly decelerated and desired positioning accuracy is attained at stationary positions around the usually mounted on a table are the several tools and unit which perform the machining operation. It is essential that all movements be completely synchronized in order to obtain desired product it is essential that all tools and units must have completed their operation and be withdrawn clear of the turret before it starts to index similarly the turret index precisely and come to rest before tools and units begin their work.

MECHANISMS:

There are a variety of index machines and this need to be selected properly to suit the given requirement. A versatile indexing unit used in presses, drilling machines has number of indexes, speed of index and dwell time which can be readily changed in this mechanism. It operates by fluid power and uses ratchet and pawl mechanism.

DESIGN OF SPECIAL PURPOSE MACHINE (SPM):-

PROBLEM DEFINITION:-

The company was using various types of milling machines like horizontal milling machine, vertical milling machine angular milling machine and HMCs the company designs and manufactures the special purpose machines needed by it in house and intended to do the same in case of milling operations. The machine will be used in milling in4 cylinder 40HP engine block of Tata motor.

The problem associated with the machine was that it was a tedious and time consuming part to mill the locus clearance in the engine block on three different machines. Also the most difficult task was to mill the portion in locus type pattern. So the machine is meant to be a rough milling machine,the clearance produced by it was not accurate and vibration produced was creating problem to the operator for achieving the required accuracy.

Also the time taken for milling operation was quite large and there was a scope in reduction of machining time so by reducing these two parameters of vibration and machining time more output could be achieved.

The above problem could be solved by designing a machine having a hydraulic type spindle having milling tool such that angular or rotational motion can be achieved. Though it will increase the cost of designing the new machine it will be nullified by reduction in machining time.

Fig. Actual working model of SPM designed and manufactured.

DESIGN PROCEDURE FOLLOWED:-

1) Design of Spindle Unit
2) Design of Spindle Shaft
3) Selection of Bearing
4) Design of Gear Box
5) Selection of Lubricants
6) Sealing of Rolling Bearing
7) Assembly procedure of spindle unit
8) Assembly procedure for Gear Box
9) Inspection after Assembly

Inputs of Machine:

SR. NO.	ENTITIES
1	Diameter of Locus clearance bore as cast (D) =30mm,to be machined
2	Cutting speed (V)= 40m/min
	Revolutions per minute (n): We Know, v= ðDn/1000 40 = ð 30 n/ 1000
3	n = 40×1000/ð 30
	n = 424.41rpm
4	Feed (f)=0.1 mm/tooth
5	Feed per minute (fm) =f×n= 42.44 mm/min
6	Depth of cut (t)= 5 mm

7	Metal removal rate (Q)=f×t×v =20 cm^3 /min
8	Approach Angle (x^0) =90^0
9	Average chip thickness (a_s) = f × sin x^0= 0.1 mm
10	Unit power (U) = 31 KW/ cm^3/min
11	Correction factor for flank wear (k_h) = 1.18
12	Side rack angleã^0 =0^0
13	Correction factor for rake angle (Kã) Kã = 1.13
14	Power at the spindle (N) =U×kh_xKã×Q = 0.826 kw
15	Efficiency of transmission (E) = 95%
16	Power of the motor (Nel) =N/E= 0.8694 kw
17	Tangential cutting force (p_z) =6120 N/V=1239.344N (1 kgf= 9.80665 N)
18	Torque at the spindle (Ts) = 975×N/n=18.6088×10^3 N-mm

Sr.No.	Parameters	Quantity
1	Working hours/shift	8
2	No. of working days in week	6
3	No. of operators	3
4	Working days per month	25

Sr.No.	Parameters	Min.
1	Machine time	12
2	Operator time	3
3	Total time/unit	15

Sr.No.	Parameters	Quantity
1	Working hours/shift	8
2	No. of working days in week	6
3	No. of operators	1
4	Working days per month	25

STANDARD TIME PER UNIT PER SHIFT PERMONTH

Sr.No.	Parameters	Min.
1	Machine time	4.12
2	Operator time	0.45
3	Total time/unit	5.3

Calculations

Machine time =4.12/0.95
=4.33
Operator time =1 min.
Total time/unit =5.33 No. of units produced/shift/month
=8×60×25/5.33
=2264 units No. of units produced per months
= 2264×3 (Three sifts per day)
= 6792 units

Opⁿ No.	Machine	Total Cycle time In min	No. of Components per month	Operators Per shift	Machining cost per unit	Machining cost per month
1	OLDSPM	17.11	2103	3	20	1, 01,880
2	NEWSPM	5.5	6792	1	15	42,060

Table No..1 Justification of new SPM locus clearance milling

Total cost saving per month : 59,820/-

Total cost saving per year : 7, 17,840/-

Fig. 2 Graphical representation of the data obtained.

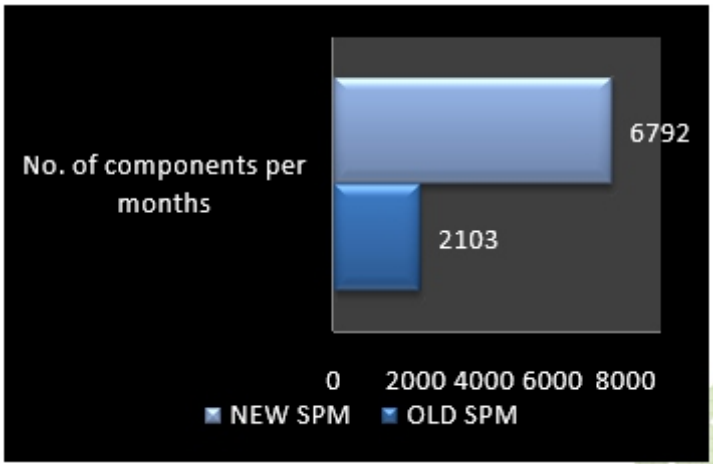

Fig. 3 Graphical representation of the data obtained.

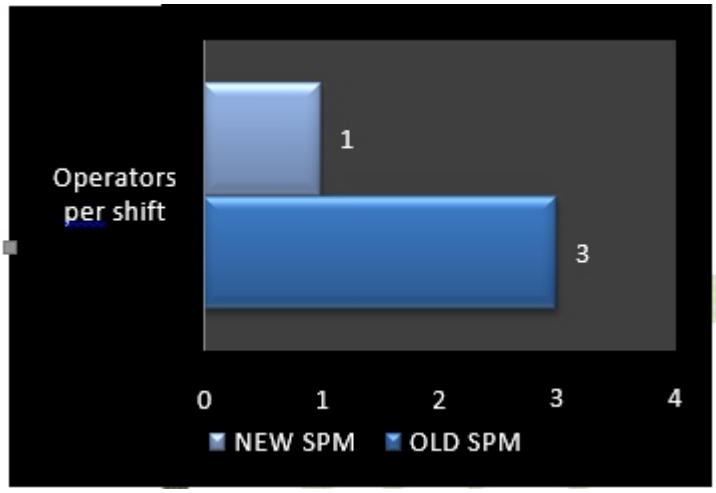

Fig. 4 Graphical representation of the data obtained.

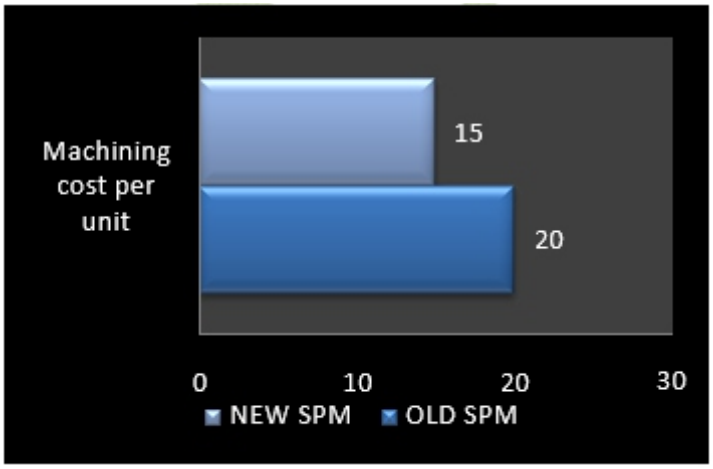

Fig. 5 Graphical representation of the data obtained.

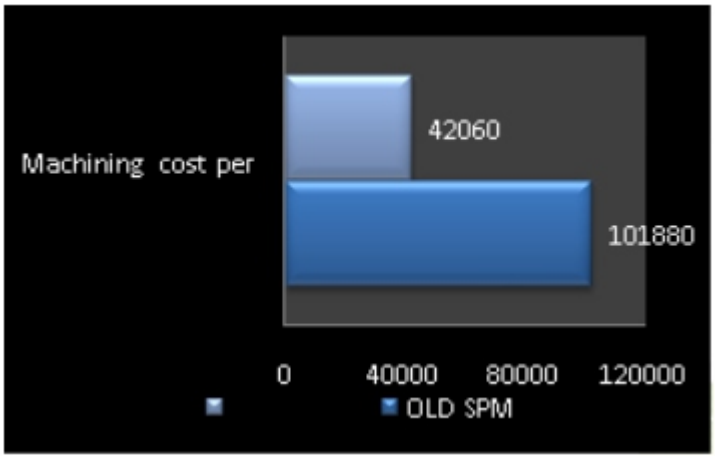

Fig. 6 Graphical representation of the data obtained.

From the overall procedure we followed in designing of the spindle unit and gear box , we conclude that design is safe , accordingly the design could be brought into practice while designing we have successive in keeping the cost factor to minimum total net savings per year after new SPM is Rs.7,17,840. Previously for the locus clearance machine three men were utilized for each machine all operation will be done on one SPM and for that one man will be required therefore saving in manpower will be 3-1= 2 men saved per day also there will be saving in space, power consumed, wages paid, handling and machining time etc.this will result into increase productivity and profit. The company can machine additional unit produced per year and meet the customers demand.

REFERENCES

[1] Machine Tool Design Handbook: Central Machine Tool Institute, Bangalore. (Tata McGraw-Hill Publishing Company Ltd. Year 2002)

[2] Design of Machine Elements: V. B. Bhandari (Tata McGraw-Hill Publishing Company Ltd. Year 2002)

[3]Machine Design: R.S. Khurmi & J.K. Gupta (S. Chand Publication Ltd. Year 1998) [4]Production Technology: R.K. Jain S.C. Gupta (Khanna Publications, New Delhi Year 1982)

Review of Heat Transfer Parameters using Internal Threaded Pipe Fitted with Inserts of Different Materials

[1] Mr. D.D.Shinde, [2] Prof. A.M. Patil, [3]Prof. H.M.Dange

[1]Department of Mechanical Engineering Shivaji University, PVPIT Budhagaon, Dist: Sangli, India
dhirajdshinde@rediffmail.com

[2]Department of Mechanical Engineering Shivaji University, PVPIT Budhagaon, Dist: Sangli, India

[3]Department of Mechanical Engineering Shivaji University, PVPIT Budhagaon, Dist: Sangli, India

ABSTRACT

Many heat transfer enhanced techniques have simultaneously been developed for the improvement of energy consumption, material saving, size reduction and pumping power reduction. Screw tape inserts in tubes are a typical technique that offers a higher heat transfer increase and, at the same time, only a mild pressure drop penalty. This study investigates the heat transfer characteristics of a horizontal tube-in-tube heat exchanger having internal threaded pipe with Screw tape inserts of different materials i.e. Mild steel screw tape and Aluminum screw tape inserted in the inner tube. Heat transfer, flow friction characteristics in a threaded tube fitted with screw tape, using oil as working fluid are investigated experimentally. Influences of the changing material i.e M.S screw tape and Aluminum screw tape arrangements are also described. The experiments are conducted using the tapes with same twist ratios and pitch over a Reynolds number range less than 2,000 in a heat exchanger.

INTRODUCTION

To achieve high heat transfer rate in an existing or new heat exchanger several techniques have been proposed in recent works. Screw tapes a type of passive heat transfer have shown good results in past studies. For experimental work different types of screw tapes of different materials of same dimensions(pitch 9mm ,depth 2.5mm, thickness of tape t= 1mm) combined with internal threaded copper pipe (ID= 13mm OD= 19mm, W= 8 mm, d= 3mm L=550 mm) have been studied. The technique of improving the performance of heat transfer system is referred to as heat transfer augmentation or intensification. This leads to reduce the size and cost of the heat exchanger. Heat transfer enhancement technology has been developed and widely applied to heat exchanger applications; for example, refrigeration, automotives, process industry, chemical industry etc. Many techniques of active and passive techniques are available for augmentation. Some common examples include steam generation, condensation in power & cogeneration plants, sensible heating and cooling inthermal processing of chemical pharmaceutical &agricultural products, fluid heating in manufacturing and waste heat recovery etc.

Laminar flow is encountered in many industrial applications. Flow of solar thermal mass of viscous oil in a parabolic trough solar collector in solar electric thermal power plant is an example. In Such case of laminar flow, there is major thermal resistance in the bulk flow in addition to the dominant thermal resistance in the thin boundary layer adjacent to the flow. Twisted-tape inserts are, therefore, used to mix the gross flow effectively in laminar flow to reduce the thermal resistance in the core flow through the helical screw inserts also tabulators. Use of heat transfer enhancement techniques lead to increase in heat transfer coefficient at the cost of increase in pressure drop, while designing a heat exchanger using any of these techniques, analysis of heat transfer rate, and to perform experimental work on considered arrangement to develop characteristics equation for predicting thermo hydraulic performance of heat exchanger.

LITERATURE REVIEW:

Hussein [1] different inlet geometries for laminar air flow combined convection heat transfer inside a horizontal circular pipe, through careful measurements, was experimentally studied under a constant wall heat flux boundary condition. It was found that the surface temperature values along the pipe dimensionless axial distance were higher for low Re number than that for high Re number due to the free convection domination on the heat transfer process.

Naphon et al. [2] studied the heat transfer characteristics and the pressure drop of the horizontal concentric tube with twisted wires brush inserts are investigated. The swirl flow is generated as fluid flowing through the plain tube with twisted wires brush insert. Due to the presence of swirl flow, the convective heat transfer obtained from the plain tube with twisted wires brush insert is higher than that with the plain tube without twisted wires brush insert. Twisted wire brushes inserts have a significant effect on the enhancement of heat transfer; however, the pressure drops also increase too.

Bhattacharyya et al. [3] presented experimental friction factor and Nusselt number data for laminar flow through a circular duct having integral transverse ribs and fitted with centre-cleared twisted-tape have been presented. Predictive friction factor and Nusselt number correlations have also been presented. The thermo hydraulic performance has been evaluated. The major findings of this experimental investigation are that the centre-cleared twisted tapes in combination with transverse ribs perform significantly better than the individual enhancement technique acting alone for laminar flow through a circular duct up to a certain amount of centre-clearance. This result is useful for the design of solar thermal heaters and heat exchangers.Chowdhury et al. [4] demonstrated An experimental study has been carried out to investigate the flow friction and heat transfer characteristics in a circular tube fitted with perforated twisted tapes of different porosities (Rp = 1.6, 4.5, 8.9 and14.7%). It has been found that the perforated twisted tape inserts enhanced the heat transfer rate significantly with corresponding increase in friction factor in comparison to that of the plain tube based on the experimental results.

Bas et al. [5] presented Heat transfer enhancement in a twisted tape inserted tube is studied experimentally in this present study. The twisted tapes are placed separately from the tube wall to obtain only heat transfer increase depending on laminar sub layer destruction near the tube wall.

Salam et al. [6] an experimental investigation was carried for measuring tube-side heat transfer coefficient, friction factor, and heat transfer enhancement efficiency of water for turbulent flow in a circular tube fitted with rectangular-cut twisted tape insert.

Saha et al. [7] had calculated experimentally friction factor and Nusselt number data for laminar flow through a circular duct having integral helical ribs and fitted with helical screw-tape inserts have been presented. Predictive friction factor and Nusselt number correlations have also been presented. The thermo hydraulic performance has been evaluated.

Remarks:

Many researchers have worked the Nusselt number, friction factor, and thermal performance factor increased with the increase of twisted wire densities.

1. Some of researchers worked on Heat transfer enhancement in a twisted tape inserted tube and convection heat transfer inside a horizontal circular pipe, through careful measurements. Very less Researchers are working on heat transfer in tube in tube heat exchanger with helical screw tape insert.

2. There is no recent work on heat transfer in tube in tube heat exchanger with helical screw tape insert for different materials also there is no any such comparison for different materials.

PROPOSED WORK:

Scope:

The scope for this study would encompass all necessary activities for benchmarking the existing application like solar power plant with the current performance level and performance standards to be set for arriving at the objectives of the dissertation work. Recommendation of the best alternative would follow the comparison of the results. Data over Testing to be shared through a Test report for the experimentation phase.

Objectives:

1. To design and manufacture internal threaded pipe, helical screw tape inserts of different materials and built up setup.
2. To perform experimental work on considered arrangement to develop characteristics equation for predicting thermo hydraulic performance of heat exchanger.
3. To study different materials of same dimension screw tape inserts at variable flow rates of oil.
4. Comparative study of proposed arrangement with and without inserts to determine the economical and thermal effectiveness.

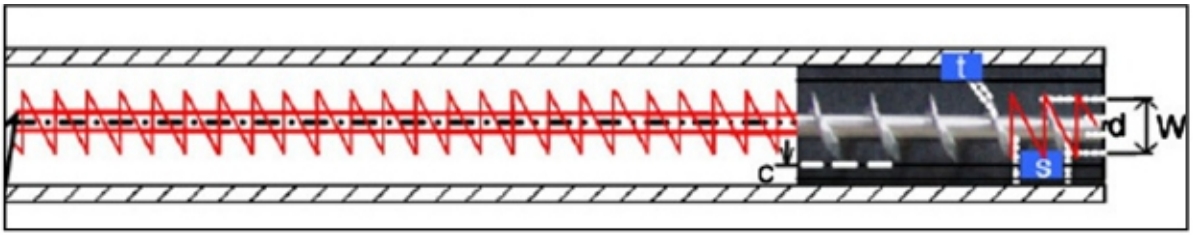

Fig. 1 Helical Screw Tape Insert (In pipe)

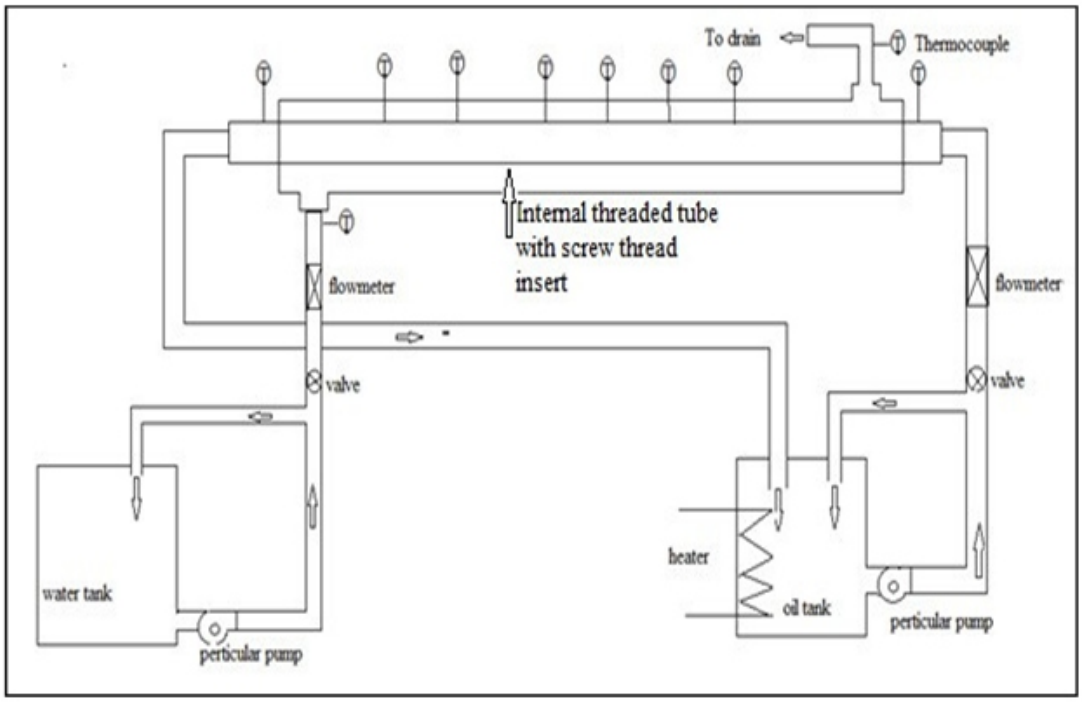

Fig.2 Experimental Setup

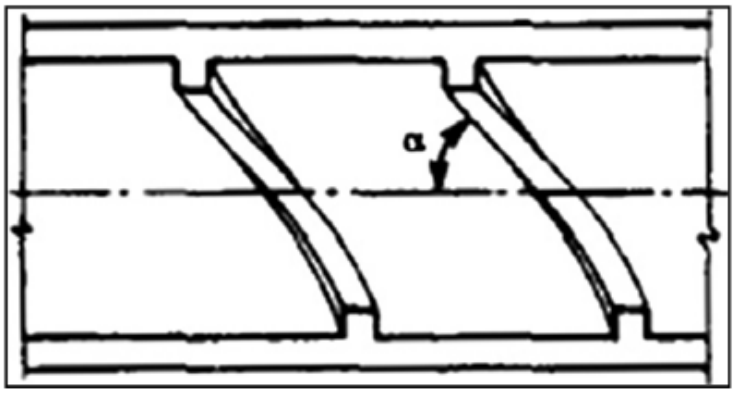

Figure.3 Internal helical Threaded Tube

Tube in Tube Heat Exchanger with Internal Threaded Pipe:

Development of test section is the main task of work here copper tube is used at the inner side of test section having 550 mm length and 13 mm inside diameter. Inside copper pipe is internally threaded (α= 600, e/Dh = 0.1026,).At the outer side pvc pipe is used having length 600 mm length and 24 mm inner diameter. And 6 thermocouples fitted on inner pipe to measure the surface temperature. At the one end of outer pipe opening for cold water and opposite end of outer pipe outlet for cold water is provided. For avoiding heat loss to surrounding heatlon insulation is wound on heat exchanger having thickness 100 mm. Engine oil is used as a hot working fluid.

CONCLUSION

The effects of the materials on the heat transfer enhancement and friction factor behaviors in laminar flow regimes (Re < 2,000) are described. The Screw tapesof MS and Aluminum insert with same dimensions (W= 8mm,d=3mm,H=9mm) at different temperatures and different cold fluid flow rates are tested using the oil as the hot working fluid and other is water.

REFERENCES

[1] Hussein A. Mohammed, "The effect of different inlet geometries on laminar flow combined convection heat transfer inside a horizontal circular pipe" Applied Thermal Engineering 29, (2009), pp. 581–590.

[2].PaisarnNaphon , TanaponSuchana,"Heat transfer enhancement and pressure drop of the horizontal concentric tube with twisted wires brush inserts" International Communications in Heat and Mass Transfer 38,(2011),pp. 236–241.

[3] Suvanjan Bhattacharyya, Sujoy Kumar Saha Experimental, "Thermo hydraulics of laminar flow through a circular tube having integral helical rib roughness and fitted with centre-cleared twisted- tape", Thermal and Fluid Science 42,(2012), pp. 154–162.

[4] M.M.K. Bhuiyaa,b, M.S.U. Chowdhury c, M. Saha d, M.T. , "Heat transfer and friction factor characteristics in turbulent flow through a tube fitted with perforated twisted tape inserts", International Communications in Heat and Mass Transfer 39 ,(2012), pp. 1505–1512.

[5] Halit Bas, Veysel Ozceyhan, "Heat transfer enhancement in a tube with twisted tape inserts placed separately from the tube wall" Experimental Thermal and Fluid Science 41, (2012), pp. 51–58.

[6] Bodius Salam, Sumana Biswas, ShuvraSaha, Muhammad Mostafa K Bhuiya," Heat transfer enhancement in a tube using rectangular-cut twisted tape insert", Procedia Engineering 56, 5th BSME International Conference on Thermal Engineering,(2013), pp. 96 – 103.

[7] SubhankarSaha, Sujoy Kumar Saha, "Enhancement of heat transfer of laminar flow of viscous oil through a circular tube having integral helical rib roughness and fitted with helical screw-tapes", Experimental Thermal and Fluid Science 47,(2013), pp. 81–89.

Instructions for Authors

Essentials for Publishing in this Journal

1 Submitted articles should not have been previously published or be currently under consideration for publication elsewhere.

2 Conference papers may only be submitted if the paper has been completely re-written (taken to mean more than 50%) and the author has cleared any necessary permission with the copyright owner if it has been previously copyrighted.

3 All our articles are refereed through a double-blind process.

4 All authors must declare they have read and agreed to the content of the submitted article and must sign a declaration correspond to the originality of the article.

Submission Process

All articles for this journal must be submitted using our online submissions system. http://enrichedpub.com/ . Please use the Submit Your Article link in the Author Service area.

Manuscript Guidelines

The instructions to authors about the article preparation for publication in the Manuscripts are submitted online, through the e-Ur (Electronic editing) system, developed by **Enriched Publications Pvt. Ltd**. The article should contain the abstract with keywords, introduction, body, conclusion, references and the summary in English language (without heading and subheading enumeration). The article length should not exceed 16 pages of A4 paper format.

Title

The title should be informative. It is in both Journal's and author's best interest to use terms suitable. For indexing and word search. If there are no such terms in the title, the author is strongly advised to add a subtitle. The title should be given in English as well. The titles precede the abstract and the summary in an appropriate language.

Letterhead Title

The letterhead title is given at a top of each page for easier identification of article copies in an Electronic form in particular. It contains the author's surname and first name initial .article title, journal title and collation (year, volume, and issue, first and last page). The journal and article titles can be given in a shortened form.

Author's Name

Full name(s) of author(s) should be used. It is advisable to give the middle initial. Names are given in their original form.

Contact Details

The postal address or the e-mail address of the author (usually of the first one if there are more Authors) is given in the footnote at the bottom of the first page.

Type of Articles

Classification of articles is a duty of the editorial staff and is of special importance. Referees and the members of the editorial staff, or section editors, can propose a category, but the editor-in-chief has the sole responsibility for their classification. Journal articles are classified as follows:

Scientific articles:

1. Original scientific paper (giving the previously unpublished results of the author's own research based on management methods).

2. Survey paper (giving an original, detailed and critical view of a research problem or an area to which the author has made a contribution visible through his self-citation);

3. Short or preliminary communication (original management paper of full format but of a smaller extent or of a preliminary character);

4. Scientific critique or forum (discussion on a particular scientific topic, based exclusively on management argumentation) and commentaries. Exceptionally, in particular areas, a scientific paper in the Journal can be in a form of a monograph or a critical edition of scientific data (historical, archival, lexicographic, bibliographic, data survey, etc.) which were unknown or hardly accessible for scientific research.

Professional articles:

1. Professional paper (contribution offering experience useful for improvement of professional practice but not necessarily based on scientific methods);
2. Informative contribution (editorial, commentary, etc.);
3. Review (of a book, software, case study, scientific event, etc.)

Language

The article should be in English. The grammar and style of the article should be of good quality. The systematized text should be without abbreviations (except standard ones). All measurements must be in SI units. The sequence of formulae is denoted in Arabic numerals in parentheses on the right-hand side.

Abstract and Summary

An abstract is a concise informative presentation of the article content for fast and accurate Evaluation of its relevance. It is both in the Editorial Office's and the author's best interest for an abstract to contain terms often used for indexing and article search. The abstract describes the purpose of the study and the methods, outlines the findings and state the conclusions. A 100- to 250-Word abstract should be placed between the title and the keywords with the body text to follow. Besides an abstract are advised to have a summary in English, at the end of the article, after the Reference list. The summary should be structured and long up to 1/10 of the article length (it is more extensive than the abstract).

Keywords

Keywords are terms or phrases showing adequately the article content for indexing and search purposes. They should be allocated heaving in mind widely accepted international sources (index, dictionary or thesaurus), such as the Web of Science keyword list for science in general. The higher their usage frequency is the better. Up to 10 keywords immediately follow the abstract and the summary, in respective languages.

Acknowledgements

The name and the number of the project or programmed within which the article was realized is given in a separate note at the bottom of the first page together with the name of the institution which financially supported the project or programmed.

Tables and Illustrations

All the captions should be in the original language as well as in English, together with the texts in illustrations if possible. Tables are typed in the same style as the text and are denoted by numerals at the top. Photographs and drawings, placed appropriately in the text, should be clear, precise and suitable for reproduction. Drawings should be created in Word or Corel.

Citation in the Text

Citation in the text must be uniform. When citing references in the text, use the reference number set in square brackets from the Reference list at the end of the article.

Footnotes

Footnotes are given at the bottom of the page with the text they refer to. They can contain less relevant details, additional explanations or used sources (e.g. scientific material, manuals). They cannot replace the cited literature.
The article should be accompanied with a cover letter with the information about the author(s): surname, middle initial, first name, and citizen personal number, rank, title, e-mail address, and affiliation address, home address including municipality, phone number in the office and at home (or a mobile phone number). The cover letter should state the type of the article and tell which illustrations are original and which are not.

Address of the Editorial Office:

Enriched Publications Pvt. Ltd.
S-9,IInd FLOOR, MLU POCKET,
MANISH ABHINAV PLAZA-II, ABOVE FEDERAL BANK,
PLOT NO-5, SECTOR -5, DWARKA, NEW DELHI, INDIA-110075,
PHONE: - + (91)-(11)-45525005

Note